Frontiers of Information Technology & Electronic Engineering
www.jzus.zju.edu.cn; engineering.cae.cn; www.springerlink.com
ISSN 2095-9184 (print); ISSN 2095-9230 (online)
E-mail: jzus@zju.edu.cn

Sum-based dynamic discrete event-triggered mechanism for synchronization of delayed neural networks under deception attacks*

Zhongjing YU†1, Duo ZHANG†‡2, Shihan KONG[1], Deqiang OUYANG[3], Hongfei LI[4], Junzhi YU†‡1

[1]*State Key Laboratory for Turbulence and Complex Systems, School of Advanced Manufacturing and Robotics, College of Engineering, Peking University, Beijing 100871, China*

[2]*Intelligent Game and Decision Laboratory, Beijing 100097, China*

[3]*College of Computer Science, Chongqing University, Chongqing 400044, China*

[4]*College of Electronic and Information Engineering, Southwest University, Chongqing 400715, China*

†E-mail: yuzhongjing@pku.edu.cn; duozhang92@std.uestc.edu.cn; junzhi.yu@ia.ac.cn

Received Nov. 12, 2024; Revision accepted Feb. 23, 2025; Crosschecked Aug. 28, 2025

Abstract: This paper focuses on the design of event-triggered controllers for the synchronization of delayed Takagi–Sugeno (T–S) fuzzy neural networks (NNs) under deception attacks. The traditional event-triggered mechanism (ETM) determines the next trigger based on the current sample, resulting in network congestion. Furthermore, such methods suffer from the issues of deception attacks and unmeasurable system states. To enhance the system stability, we adaptively detect the occurrence of events over a period of time. In addition, deception attacks are recharacterized to describe general scenarios. Specifically, the following enhancements are implemented: First, we use a Bernoulli process to model the occurrence of deception attacks, which can describe a variety of attack scenarios as a type of general Markov process. Second, we introduce a sum-based dynamic discrete event-triggered mechanism (SDDETM), which uses a combination of past sampled measurements and internal dynamic variables to determine subsequent triggering events. Finally, we incorporate a dynamic output feedback controller (DOFC) to ensure the system stability. The concurrent design of the DOFC and SDDETM parameters is achieved through the application of the cone complement linearization (CCL) algorithm. We further perform two simulation examples to validate the effectiveness of the algorithm.

Key words: Sum-based dynamic discrete event-triggered mechanism; Takagi–Sugeno (T–S) fuzzy model; Deception attacks

https://doi.org/10.1631/FITEE.2401000 **CLC number:** TP273

1 Introduction

Synchronization of neural networks (NNs), as an important method, has received extensive research in recent years for NN-based control. In the network environment, the transmission of a large amount of information for controlling NNs leads to network congestion (Wang et al., 2021), making it more difficult for NNs to synchronize. Worse, network attacks (Ma et al., 2024) as well as unmeasurable system state (Liang and Huang, 2021) problems further come up, resulting in deterioration of the system performance.

For the problem of network congestion, the event-triggered mechanism (ETM) is an effective solution to alleviate the issue. However, designing

‡ Corresponding authors

* Project supported by the National Natural Science Foundation of China (Nos. T2121002, 62473321, 62403014, and 62233001)

ORCID: Zhongjing YU, https://orcid.org/0000-0003-4128-5877; Duo ZHANG, https://orcid.org/0000-0003-4895-2636; Shihan KONG, https://orcid.org/0000-0002-6714-1313; Deqiang OUYANG, https://orcid.org/0000-0003-2259-886X; Hongfei LI, https://orcid.org/0000-0002-9816-717X; Junzhi YU, https://orcid.org/0000-0002-6347-572X

event-triggering conditions in a continuous space is a significant challenge (Liu ZQ et al., 2022; Zhang D et al., 2023). Shen et al. (2023) designed a dynamic ETM with a dynamic threshold parameter (DTP) that can adaptively adjust the triggering condition based on the evolution of system states. This allows the triggering condition to be more responsive to the current system state. Bao et al. (2024) proposed a Lyapunov function-based ETM and a sampled-data-based ETM to reduce network data transmission. The former introduces a waiting time to avoid unnecessary frequent transmission, and incorporates an acknowledgment mechanism to promptly transmit data. The latter is to check the triggering condition only at sampling instants. Lei et al. (2024) designed an ETM to ensure the existence of a strictly positive minimum interevent time, thereby preventing Zeno behavior (a phenomenon where an infinite number of triggers occur in a finite time interval in event-triggered control systems) and reducing unnecessary sampling and control updates. Liu YJ et al. (2023) compared the difference between the current error and the error at the last transmission. Data are only sent when the difference exceeds the threshold. However, these mechanisms often rely on the current state of the system to determine the next trigger, which can lead to high trigger frequency and potential Zeno behavior. This can significantly degrade the performance of the system and increase the computational and communication overhead. Consequently, this results in ineffective event filtering, and fails to reach the trade-off between the network transmission efficiency and information integrity.

Moreover, in many practical applications, the system states are often unmeasurable. The communication network is vulnerable to external malicious attacks due to its openness, sharing, interconnectivity, and versatility. Control becomes challenging, especially in the case of the system being subject to uncertainties and nonlinearities, along with corrupted or incomplete state information. This vulnerability can lead to a serious degradation of the system performance, and may even cause a system crash. Takagi–Sugeno (T–S) fuzzy NNs (Liu JL et al., 2019a; Yan et al., 2019; Tan et al., 2020) have emerged and been widely studied. Nevertheless, the issue of synchronizing T–S fuzzy NNs in the face of cyberattacks has not been extensively explored. Based on this motivation, this paper designs a dynamic output feedback controller (DOFC) for the T–S fuzzy NN system to counteract deception attacks.

In addition, avoiding Zeno behavior (Wen et al., 2016, 2018) is a critical criterion in event-triggered control systems. This behavior can lead to several adverse effects, including excessive computational resource consumption and potential system instability. To significantly save communication resources, this study integrates an internal dynamic variable into the sum-based ETM, hereby designated as the sum-based dynamic discrete event-triggered mechanism (SDDETM). To address the above challenges, we employ fuzzy networks. These networks possess robust fuzzy inference capabilities. We leverage these capabilities to model and analyze complex systems. Fuzzy networks are capable of attaining more accurate predictions, identification, and control when confronted with nonlinear, time-variant, and uncertain issues. In contrast to traditional ETM, SDDETM can decrease the trigger frequency, thereby enhancing the performance of ETM. Considering these advancements, the principal contributions are shown as follows:

1. The triggering condition of the proposed SDDETM is composed of two parts: the combination of multiple previous measurement samples and the inclusion of an inherent dynamic variable. With this SDDETM approach, Zeno behavior can be easily excluded.

2. Different from traditional methods which use the Bernoulli distribution to characterize deception attacks, we regard the attack process as a Markov process, and therefore, adopt the Bernoulli process to characterize the occurrence of deceptive attacks.

3. A DOFC is proposed to ensure the stability of the T–S fuzzy NN system. Both communication channels from the sensor to DOFC and DOFC to zero-order hold (ZOH) are subject to stochastic deception attacks.

Notations The symbol "$*$" denotes the symmetric counterparts within a symmetric matrix. The notation "$[*]\boldsymbol{U}\boldsymbol{x}$" is employed to encapsulate the quadratic form, specifically, $[*]\boldsymbol{U}\boldsymbol{x} = \boldsymbol{x}^{\mathrm{T}}\boldsymbol{U}\boldsymbol{x}$. $\mathrm{He}(\boldsymbol{A}) \triangleq \boldsymbol{A}^{\mathrm{T}} + \boldsymbol{A}$. $\mathbb{R}^p$ denotes the p-dimensional Euclidean space, and $\mathbb{R}^{p\times q}$ is the set of real $p \times q$ matrices. $\mathcal{N}_{m+}$ and $\mathcal{N}_m$ denote the set of positive integers from 1 to m and non-negative integers from 0 to m, respectively. $\mathcal{S}_n^+$ denotes the collection of

$n \times n$ symmetric positive definite matrices.

2 System formulation

Fig. 1 depicts the schematic representation of the delayed T-S fuzzy NNs subjected to deception attacks. Each part of the diagram is introduced in detail in the following subsections.

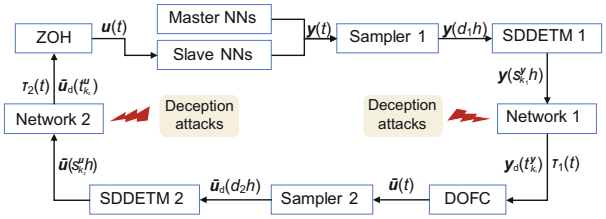

Fig. 1 System schematic representation of the NNs

2.1 T–S fuzzy NN model

The inferred time-delay T–S fuzzy NNs with M plant rule nonlinear systems are described as

Plant rule l: if $\theta_1(t)$ denotes υ_1^l, $\cdots$, $\theta_k(t)$ denotes υ_k^l, then

$$\begin{cases} \dot{\boldsymbol{x}}_{\mathrm{m}}(t) = \boldsymbol{A}_l \boldsymbol{x}_{\mathrm{m}}(t) + \boldsymbol{B}_l \mathscr{F}(\boldsymbol{x}_{\mathrm{m}}(t)) \\ \qquad\qquad + \boldsymbol{C}_l \mathscr{F}(\boldsymbol{x}_{\mathrm{m}}(t-h(t))) + \boldsymbol{\mathcal{I}}, \\ \boldsymbol{y}_{\mathrm{m}}(t) = \boldsymbol{D}_l \boldsymbol{x}_{\mathrm{m}}(t), \end{cases}$$

where $\boldsymbol{x}_{\mathrm{m}}(t) = \mathrm{col}\{x_{\mathrm{m}1}(t), x_{\mathrm{m}2}(t), \cdots, x_{\mathrm{m}a}(t)\} \in \mathbb{R}^a$ and $\boldsymbol{y}_{\mathrm{m}}(t) \in \mathbb{R}^c$ denote the state vector and the measurable output in the master system, respectively. The system matrices $\boldsymbol{A}_l$, $\boldsymbol{B}_l$, $\boldsymbol{C}_l \in \mathbb{R}^{a\times a}$, and $\boldsymbol{D}_l \in \mathbb{R}^{c\times a}$ are known, and $\boldsymbol{\mathcal{I}} \in \mathbb{R}^a$ represents the input bias. The function $\mathscr{F}()$ represents the neuron activation function. The vector $\boldsymbol{\theta} = [\theta_1(t), \theta_2(t), \cdots, \theta_k(t)] \in \mathbb{R}^k$ denotes k premise variables. υ_k^l, $l \in \mathcal{N}_L$, is the fuzzy set, where L represents the count of IF-THEN rules.

Similarly, the slave system is defined as follows:

Plant rule l: if $\theta_1(t)$ denotes υ_1^l, $\cdots$, $\theta_k(t)$ denotes υ_k^l, then

$$\begin{cases} \dot{\boldsymbol{x}}_{\mathrm{s}}(t) = \boldsymbol{A}_l \boldsymbol{x}_{\mathrm{s}}(t) + \boldsymbol{B}_l \mathscr{F}(\boldsymbol{x}_{\mathrm{s}}(t)) + \boldsymbol{C}_l \mathscr{F}(\boldsymbol{x}_{\mathrm{s}}(t-h(t))) \\ \qquad\qquad + \boldsymbol{E}_l \boldsymbol{u}(t, r_t, q_t) + \boldsymbol{\mathcal{I}}, \\ \boldsymbol{y}_{\mathrm{s}}(t) = \boldsymbol{D}_l \boldsymbol{x}_{\mathrm{s}}(t), \end{cases}$$

where $\boldsymbol{x}_{\mathrm{s}}(t)$ and $\boldsymbol{y}_{\mathrm{s}}(t)$ represent the state vector and measurable output of the response in the slave system, respectively. The control input is represented by $\boldsymbol{u}(t, r_t, q_t)$ with r_t referring to the deception attack to Network 1 at time t and q_t referring to the deception attack to Network 2 at time t, and $\boldsymbol{E}_l$ is the input matrix. Through fuzzy aggregation, the T–S fuzzy master and slave systems can be formulated in the following manner:

$$\begin{cases} \dot{\boldsymbol{x}}_{\mathrm{m}}(t) = \sum\limits_{l=1}^{L} h_l(\boldsymbol{\theta}(t))[\boldsymbol{A}_l \boldsymbol{x}_{\mathrm{m}}(t) + \boldsymbol{B}_l \mathscr{F}(\boldsymbol{x}_{\mathrm{m}}(t)) \\ \qquad\qquad + \boldsymbol{C}_l \mathscr{F}(\boldsymbol{x}_{\mathrm{m}}(t-h(t))) + \boldsymbol{\mathcal{I}}], \\ \boldsymbol{y}_{\mathrm{m}}(t) = \sum\limits_{l=1}^{L} h_l(\boldsymbol{\theta}(t)) \boldsymbol{D}_l \boldsymbol{x}_{\mathrm{m}}(t), \end{cases} \tag{1}$$

$$\begin{cases} \dot{\boldsymbol{x}}_{\mathrm{s}}(t) = \sum\limits_{l=1}^{L} h_l(\boldsymbol{\theta}(t))[\boldsymbol{A}_l \boldsymbol{x}_{\mathrm{s}}(t) + \boldsymbol{B}_l \mathscr{F}(\boldsymbol{x}_{\mathrm{s}}(t)) \\ \qquad\qquad + \boldsymbol{C}_l \mathscr{F}(\boldsymbol{x}_{\mathrm{s}}(t-h(t))) + \boldsymbol{E}_l \boldsymbol{u}(t, r_t, q_t) + \boldsymbol{\mathcal{I}}], \\ \boldsymbol{y}_{\mathrm{s}}(t) = \sum\limits_{l=1}^{L} h_l(\boldsymbol{\theta}(t)) \boldsymbol{D}_l \boldsymbol{x}_{\mathrm{s}}(t), \end{cases} \tag{2}$$

where $h(t)$ is the time-varying delay, and function $h_l(\boldsymbol{\theta}(t)) = \frac{\mu_l(\boldsymbol{\theta}(t))}{\sum_{l=1}^{L} \mu_l(\boldsymbol{\theta}(t))}$, $0 \le h_l(\boldsymbol{\theta}(t)) \le 1$, $\sum\limits_{l=1}^{M} h_l(\boldsymbol{\theta}(t)) = 1$, $\mu_l(\boldsymbol{\theta}(t)) = \Pi_{d=1}^{k} \varrho_d^l(\boldsymbol{\theta}(t))$, and $\varrho_d^l(\boldsymbol{\theta}(t))$ is the grade of membership function of $\boldsymbol{\theta}(t)$ in υ_d^l with d being the conjugate variable (Zadeh, 1968).

From Eqs. (1) and (2), the synchronization error system is represented as follows:

$$\begin{cases} \dot{\boldsymbol{x}}_{\mathrm{e}}(t) = \sum\limits_{l=1}^{L} h_l(\boldsymbol{\theta}(t))[\boldsymbol{A}_l \boldsymbol{x}_{\mathrm{e}}(t) + \boldsymbol{B}_l \boldsymbol{\varphi}(\boldsymbol{x}_{\mathrm{e}}(t)) \\ \qquad\qquad + \boldsymbol{C}_l \boldsymbol{\varphi}(\boldsymbol{x}_{\mathrm{e}}(t-h(t))) + \boldsymbol{E}_l \boldsymbol{u}(t, r_t, q_t)], \\ \boldsymbol{y}(t) = \sum\limits_{l=1}^{L} h_l(\boldsymbol{\theta}(t)) \boldsymbol{D}_l \boldsymbol{x}_{\mathrm{e}}(t), \end{cases}$$

where $\boldsymbol{x}_{\mathrm{e}}(t) = \boldsymbol{x}_{\mathrm{s}}(t) - \boldsymbol{x}_{\mathrm{m}}(t)$, $\boldsymbol{\varphi}(\boldsymbol{x}_{\mathrm{e}}(t)) = \mathscr{F}(\boldsymbol{x}_{\mathrm{s}}(t)) - \mathscr{F}(\boldsymbol{x}_{\mathrm{m}}(t))$, and $\boldsymbol{\varphi}(\boldsymbol{x}_{\mathrm{e}}(t-h(t))) = \mathscr{F}(\boldsymbol{x}_{\mathrm{s}}(t-h(t))) - \mathscr{F}(\boldsymbol{x}_{\mathrm{m}}(t-h(t)))$.

2.2 SDDETM

The communication link between the sampler and the DOFC (sampler–DOFC) is referred to as Network 1, and the channel connecting the DOFC

to the ZOH (DOFC–ZOH) is named Network 2. The sampler operates with a sampling period of h. The output of the two samplers consists of the data packet series $[d_1, \boldsymbol{y}(d_1h)]$ and $[d_2, \bar{\boldsymbol{u}}_{\mathrm{d}}(d_2h)]$, where $d_1, d_2 \in \mathbb{N}^+$, and $\bar{\boldsymbol{u}}(\cdot)$ is the discrete-time control signal through a ZOH operation. The delays that vary over time in Networks 1 and 2 are indicated by $\tau_1(t) \in [0, \tau_{1_{\mathrm{M}}}]$ and $\tau_2(t) \in [0, \tau_{2_{\mathrm{M}}}]$, respectively, with $\tau_{1_{\mathrm{M}}}, \tau_{2_{\mathrm{M}}} \in \mathbb{R}^+$. Here M denotes the maximum value. To design the SDDETM, we make the following assumptions:

Assumption 1 In the NNs, data transmissions over the networks are in a single-packet form. There exist time delays, but there are no packet dropouts or disorders in the communication networks.

This assumption simplifies the analysis by avoiding the complexities introduced by packet dropouts or disorders, which is common in practical networked control systems. This assumption is widely used in literature to focus on the impact of time delays.

Assumption 2 The adversary attempts to deteriorate the controller performance by injecting a deception signal into the sampler–DOFC and DOFC–ZOH communication channels. Specifically, the deception signal is modeled as nonlinear functions $\boldsymbol{G}_{\mathrm{s}}(\boldsymbol{y}(t))$ and $\boldsymbol{G}_{\mathrm{c}}(\bar{\boldsymbol{u}}(t))$, which satisfy the following conditions:

$$\begin{aligned} &\|\boldsymbol{G}_{\mathrm{s}}(\boldsymbol{y}(t))\| \le \|\boldsymbol{G}_{\mathrm{s}}\boldsymbol{y}(t)\|, \qquad \boldsymbol{G}_{\mathrm{s}}^{\mathrm{T}}\boldsymbol{G}_{\mathrm{s}} > 0, \\ &\|\boldsymbol{G}_{\mathrm{c}}(\bar{\boldsymbol{u}}(t))\| \le \|\boldsymbol{G}_{\mathrm{c}}\bar{\boldsymbol{u}}(t)\|, \qquad \boldsymbol{G}_{\mathrm{c}}^{\mathrm{T}}\boldsymbol{G}_{\mathrm{c}} > 0, \end{aligned}$$

where $\boldsymbol{G}_{\mathrm{s}}$ and $\boldsymbol{G}_{\mathrm{c}}$ are known matrices that characterize the deception attacks to Networks 1 and 2 respectively, and the functions $\boldsymbol{G}_{\mathrm{s}}(\boldsymbol{y}(t))$ and $\boldsymbol{G}_{\mathrm{c}}(\bar{\boldsymbol{u}}(t))$ represent the nonlinearities introduced by the attacks.

This assumption is realistic in the context of networked control systems, where communication channels are vulnerable to attacks. Deception attacks are a common type of cyberattack that can significantly degrade system performance.

Assumption 3 Referring to Song et al. (2019), for any $x_1, x_2 \in \mathbb{R}$, $\mathscr{A} = 1, 2, \cdots, a$, the activation function $\mathscr{F}()$ satisfies the following condition:

$$\mathscr{K}_{\mathscr{A}}^- \le \frac{\mathscr{F}_{\mathscr{A}}(x_1) - \mathscr{F}_{\mathscr{A}}(x_2)}{x_1 - x_2} \le \mathscr{K}_{\mathscr{A}}^+. \tag{3}$$

Here, $\mathscr{K}_{\mathscr{A}}^-$ and $\mathscr{K}_{\mathscr{A}}^+$ are predetermined scalars. For convenience, we define $\boldsymbol{\mathscr{K}}_{\mathrm{m}} = \mathrm{diag}\{\mathscr{K}_1^-, \mathscr{K}_2^-, \ldots, \mathscr{K}_a^-\}$, $\boldsymbol{\mathscr{K}}_{\mathrm{M}} = \mathrm{diag}\{\mathscr{K}_1^+, \mathscr{K}_2^+, \ldots, \mathscr{K}_a^+\}$ with m and M defining the minimum and maximum values of the matrix, respectively.

This assumption ensures that the activation functions are Lipschitz continuous, which is a common requirement in the analysis of NNs. It allows us to derive stability conditions and design controllers that can handle the nonlinearities introduced by the activation functions.

The SDDETM is implemented for both Networks 1 and 2, designated as SDDETMs 1 and 2, respectively. Within SDDETM 1, let $\boldsymbol{y}(s_{k_1}^{\boldsymbol{y}}h)$ denote the most recent sample that has been effectively sent through Network 1, and $\boldsymbol{y}(d_1h)$ denote the most recent sampled data. We establish the following criterion to identify the next triggering moment:

$$s_{k_1+1}^{\boldsymbol{y}}h = \min_{d_1 \in \mathbb{N}^+} \{d_1h > s_{k_1}^{\boldsymbol{y}}h \mid \mathbb{A}_1(t) \ge 0\}, \tag{4}$$

with

$$\begin{aligned} \mathbb{A}_1(t) =& \sum_{i=0}^{N_1} [\boldsymbol{e}_{1_i}^{\mathrm{T}}(t)\boldsymbol{\Phi}_{1_i}\boldsymbol{e}_{1_i}(t) - \epsilon_{1_i}\boldsymbol{y}^{\mathrm{T}}(d_1h - ih) \\ & \cdot \boldsymbol{\Phi}_{1_i}\boldsymbol{y}(d_1h - ih)] - \frac{1}{\kappa_1}\eta_1(t), \\ \boldsymbol{e}_{1_i}(t) =& \boldsymbol{y}(s_{k_1}^{\boldsymbol{y}}h - ih) - \boldsymbol{y}(d_1h - ih), i \in \mathcal{N}_{N_1}, \end{aligned}$$

where $\epsilon_{1_i}, \kappa_1 \in \mathbb{R}^+$, $N_1 \ge 0$, $\boldsymbol{\Phi}_{1_i}$ represents the positive matrix that needs to be constructed.

In Eq. (4), $\eta_1(t)$ is generated by

$$\begin{aligned} &\dot{\eta}_1(t) \\ =& -\mu_1\eta_1(t) + \sum_{i=0}^{N_1} [\epsilon_{1_i}\boldsymbol{y}^{\mathrm{T}}(d_1h - ih)\boldsymbol{\Phi}_{1_i}\boldsymbol{y}(d_1h - ih) \\ & - \boldsymbol{e}_{1_i}^{\mathrm{T}}(t)\boldsymbol{\Phi}_{1_i}\boldsymbol{e}_{1_i}(t)], \end{aligned}$$

where $\mu_1 > 0$ and $\eta_1(s_0^{\boldsymbol{y}}h) = 0$ are the given parameter and the initial condition, respectively.

Similarly, for SDDETM 2, we have

$$s_{k_2+1}^{\boldsymbol{u}}h = \min_{d_2 \in \mathbb{N}^+} \{d_2h > s_{k_2}^{\boldsymbol{u}}h \mid \mathbb{A}_2(t) \ge 0\}, \tag{5}$$

where

$$\begin{aligned}\mathbb{A}_2(t)=&\sum_{j=0}^{N_2}[\boldsymbol{e}_{2_j}^{\mathrm{T}}(t)\boldsymbol{\Phi}_{2_j}\boldsymbol{e}_{2_j}(t)-\epsilon_{2_j}\bar{\boldsymbol{u}}^{\mathrm{T}}(d_2h-jh)\\&\cdot\boldsymbol{\Phi}_{2_j}\bar{\boldsymbol{u}}(d_2h-jh)]-\frac{1}{\kappa_2}\eta_2(t),\\\boldsymbol{e}_{2_j}(t)=&\bar{\boldsymbol{u}}(s_{k_2}^{\boldsymbol{u}}h-jh)-\bar{\boldsymbol{u}}(d_2h-jh),j\in\mathcal{N}_{N_2},\\\dot{\eta}_2(t)=&-\mu_2\eta_2(t)+\sum_{j=0}^{N_2}[\epsilon_{2_i}\bar{\boldsymbol{u}}^{\mathrm{T}}(d_2h-jh)\\&\cdot\boldsymbol{\Phi}_{2_j}\bar{\boldsymbol{u}}(d_2h-jh)-\boldsymbol{e}_{2_j}^{\mathrm{T}}(t)\boldsymbol{\Phi}_{2_j}\boldsymbol{e}_{2_j}(t)].\end{aligned}$$

From Eqs. (4) and (5), we conclude that the SDDETM considers both the latest sample measurement and several previous ones. By modifying the parameters N_1 and N_2, the count of samples considered for determining the subsequent triggering instant can be adjusted.

Remark 1 The proposed SDDETM exhibits some advantages over traditional ETMs: It requires no additional hardware for monitoring the continuous measurements, thereby reducing computational energy for the sensor units (Donkers and Heemels, 2012; Zhang LR et al., 2021). In contrast to the periodic ETMs (Heemels et al., 2013; Guo et al., 2014; Zhang XM and Han, 2014), the SDDETM integrates a broader spectrum of system information to decide the sequential triggers by incorporating historical samples. The infamous Zeno behavior that needs intricate analysis (Yan et al., 2019; Zhang LR et al., 2020) can be readily excluded due to the discrete nature of the SDDETM. It is present within a broader framework that encompasses the periodic ETMs (Guo et al., 2014; Zhang XM and Han, 2014) as a specific instance when $N_1=N_2=0$. Through the incorporation of internal dynamic variables, the SDDETM increases the minimum operation time for event triggering, and further improves the efficiency of network communications.

2.3 Deception attacks

During data transmission, deception attacks are factored into the analysis, which compromises the veracity and reliability of packets through the manipulation of their contents. We postulate that the adversaries have the capability to capture the transmitted data and substitute them with deceptive content. Inspired by Liu JL et al. (2018, 2019b), we model the malicious signal within sensor–DOFC and DOFC–ZOH as a nonlinear function, denoted as $\boldsymbol{\mathcal{G}}(\boldsymbol{y}(t))$ and $\boldsymbol{\mathcal{G}}(\bar{\boldsymbol{u}}(t))$, respectively.

Let $\{r(t)\}_{t\geq0}$ and $\{q(t)\}_{t\geq0}$ denote two distinct right-continuous Markov processes, each taking values within the set $\mathcal{G}=\{1,2\}$. These processes are dominated by their generators, denoted as $\boldsymbol{\pi}=[\pi_{\mathscr{M}\mathscr{N}}]_{2\times2}$ and $\boldsymbol{\rho}=[\rho_{\mathscr{P}\mathscr{Q}}]_{2\times2}$. The transition probabilities are given by (Kazemy et al., 2022)

$$\Pr\{r_{t+\delta}=\mathscr{N}|r_t=\mathscr{M}\}=\begin{cases}\pi_{\mathscr{M}\mathscr{N}}\delta+o(\delta),\ \mathscr{M}\neq\mathscr{N},\\1+\pi_{\mathscr{M}\mathscr{M}}\delta+o(\delta),\ \mathscr{M}=\mathscr{N},\end{cases}$$

$$\Pr\{q_{t+\delta}=\mathscr{Q}|q_t=\mathscr{P}\}=\begin{cases}\rho_{\mathscr{P}\mathscr{Q}}\delta+o(\delta),\ \mathscr{P}\neq\mathscr{Q},\\1+\rho_{\mathscr{P}\mathscr{P}}\delta+o(\delta),\ \mathscr{P}=\mathscr{Q}.\end{cases}$$

Here, $\delta>0$, $o(\delta)$ denotes the higher-order infinitesimal of δ, $\pi_{\mathscr{M}\mathscr{N}}\geq0$ ($\mathscr{M}\neq\mathscr{N}$), and $\rho_{\mathscr{P}\mathscr{Q}}\geq0$ ($\mathscr{P}\neq\mathscr{Q}$), with $\pi_{\mathscr{M}\mathscr{M}}=-\sum_{\mathscr{M}\neq\mathscr{N}}\pi_{\mathscr{M}\mathscr{N}}$, and $\rho_{\mathscr{P}\mathscr{P}}=-\sum_{\mathscr{P}\neq\mathscr{Q}}\rho_{\mathscr{P}\mathscr{Q}}$, for any $\mathscr{M},\mathscr{P}\in\mathcal{G}$.

For DOFC, due to the attacks on the communication network during data transmission, the input consists of triggered measurements.

$$\boldsymbol{y}_{\mathrm{d}}(s_{k_1}^{\boldsymbol{y}}h)=b^{\mathrm{s}}(r_t)\boldsymbol{y}(s_{k_1}^{\boldsymbol{y}}h)+(1-b^{\mathrm{s}}(r_t))\boldsymbol{\mathcal{G}}_{\mathrm{s}}(\boldsymbol{y}(s_{k_1}^{\boldsymbol{y}}h)),\tag{6}$$

where $\boldsymbol{\mathcal{G}}_{\mathrm{s}}$ represents the function of characterizing deception attacks within the sampler–DOFC, satisfying $\|\boldsymbol{\mathcal{G}}_{\mathrm{s}}(\boldsymbol{y}(t))\|\leq\|\boldsymbol{G}_{\mathrm{s}}\boldsymbol{y}(t)\|$ with $\boldsymbol{G}_{\mathrm{s}}^{\mathrm{T}}\boldsymbol{G}_{\mathrm{s}}>0$, $b^{\mathrm{s}}(1)=1$, and $b^{\mathrm{s}}(2)=0$.

Similarly, we have the form of the real control input:

$$\bar{\boldsymbol{u}}_{\mathrm{d}}(s_{k_2}^{\boldsymbol{u}}h)=b^{\mathrm{c}}(q_t)\bar{\boldsymbol{u}}(s_{k_2}^{\boldsymbol{u}}h)+(1-b^{\mathrm{c}}(q_t))\boldsymbol{\mathcal{G}}_{\mathrm{c}}(\bar{\boldsymbol{u}}(s_{k_{\mathrm{c}}}^{\boldsymbol{u}}h)),\tag{7}$$

where $\boldsymbol{\mathcal{G}}_{\mathrm{c}}$ denotes the function that characterizes deception attacks within the DOFC–ZOH, satisfying $\|\boldsymbol{\mathcal{G}}_{\mathrm{c}}(\bar{\boldsymbol{u}}(t))\|\leq\|\boldsymbol{G}_{\mathrm{c}}\bar{\boldsymbol{u}}(t)\|$ with $\boldsymbol{G}_c^{\mathrm{T}}\boldsymbol{G}_{\mathrm{c}}>0$, $b^{\mathrm{c}}(1)=1$, and $b^{\mathrm{c}}(2)=0$.

2.4 T–S fuzzy DOFC

Let $t_{k_1}^{\boldsymbol{y}}/t_{k_2}^{\boldsymbol{u}}$ represents the time series at which the DOFC/ZOH acquires the triggered sample, with $k_1/k_2\in\mathbb{N}^+$. Taking into account the influence of the time delay, we obtain

$$\begin{aligned}\boldsymbol{y}_{\mathrm{d}}(t_{k_1}^{\boldsymbol{y}})&=\boldsymbol{y}_{\mathrm{d}}(s_{k_1}^{\boldsymbol{y}}h),\ t\in[t_{k_1}^{\boldsymbol{y}},t_{k_1+1}^{\boldsymbol{y}}),\\\bar{\boldsymbol{u}}_{\mathrm{d}}(t_{k_2}^{\boldsymbol{u}})&=\bar{\boldsymbol{u}}_{\mathrm{d}}(s_{k_2}^{\boldsymbol{u}}h),\ t\in[t_{k_2}^{\boldsymbol{u}},t_{k_2+1}^{\boldsymbol{u}}).\end{aligned}$$

Define

$$\begin{aligned}
&\phi_{k_1} \triangleq \min\{o_{\boldsymbol{y}} \mid t^{\boldsymbol{y}}_{k_1} + o_{\boldsymbol{y}} h \geq t^{\boldsymbol{y}}_{k_1+1},\ o_{\boldsymbol{y}} \in \mathbb{N}^+\},\\
&\phi_{k_2} \triangleq \min\{o_{\boldsymbol{u}} \mid t^{\boldsymbol{u}}_{k_2} + o_{\boldsymbol{u}} h \geq t_{k_2+1},\ o_{\boldsymbol{u}} \in \mathbb{N}^+\},\\
&\mathcal{B}_{k_{\boldsymbol{y}}} = [t^{\boldsymbol{y}}_{k_1} + (k_{\boldsymbol{y}} - 1)h, t^{\boldsymbol{y}}_{k_1} + k_{\boldsymbol{y}} h),\\
&k_{\boldsymbol{y}} = 1, 2, \cdots, \phi_{k_1} - 1,\\
&\mathcal{B}_{\phi_{k_1}} = [t^{\boldsymbol{y}}_{k_1} + (\phi_{k_1} - 1)h, t^{\boldsymbol{y}}_{k_1+1}),\\
&\mathcal{C}_{k_{\boldsymbol{u}}} = [t^{\boldsymbol{u}}_{k_2} + (k_{\boldsymbol{u}} - 1)h, t^{\boldsymbol{u}}_{k_2} + k_{\boldsymbol{u}} h),\\
&k_{\boldsymbol{u}} = 1, 2, \cdots, \phi_{k_2} - 1,\\
&\mathcal{C}_{\phi_{k_2}} = [t_{k_2} + (\phi_{k_2} - 1)h,\ t^{\boldsymbol{u}}_{k_2+1}).
\end{aligned}$$

Subsequently, the interevent interval $[t^{\boldsymbol{y}}_{k_1}, t^{\boldsymbol{y}}_{k_1+1})$ and $[t^{\boldsymbol{u}}_{k_2}, t^{\boldsymbol{u}}_{k_2+1})$ can be represented as follows:

$$[t^{\boldsymbol{y}}_{k_1}, t^{\boldsymbol{y}}_{k_1+1}) = \cup_{k_{\boldsymbol{y}}=1}^{\phi_{k_1}} \mathcal{B}_{k_{\boldsymbol{y}}},\ [t^{\boldsymbol{u}}_{k_2}, t^{\boldsymbol{u}}_{k_2+1}) = \cup_{k_{\boldsymbol{u}}=1}^{\phi_{k_2}} \mathcal{B}_{k_{\boldsymbol{u}}}. \tag{8}$$

We further define some "artificial" functions $\delta_{1_i}(t)$ ($\delta_{2_j}(t)$) and $\boldsymbol{e}_{1_i}(t)$ ($\boldsymbol{e}_{2_j}(t)$) where $i \in \mathcal{N}_{N_1}$ and $j \in \mathcal{N}_{N_2}$, on $[t^{\boldsymbol{y}}_{k_1}, t^{\boldsymbol{y}}_{k_1+1})$ ($[t^{\boldsymbol{u}}_{k_2}, t^{\boldsymbol{u}}_{k_2+1})$).

$$\delta_{1_i}(t) \triangleq \begin{cases} t - (s^{\boldsymbol{y}}_{k_1} - i)h, & t \in \mathcal{B}_1,\\ t - (s^{\boldsymbol{y}}_{k_1} - i)h - h, & t \in \mathcal{B}_2,\\ \quad\vdots & \quad\vdots\\ t - (s^{\boldsymbol{y}}_{k_1} - i)h - (\phi_{k_1} - 1)h, & t \in \mathcal{B}_{\phi_{k_1}}, \end{cases} \tag{9}$$

$$\boldsymbol{e}_{1_i}(t) \triangleq \begin{cases} \boldsymbol{y}[(s^{\boldsymbol{y}}_{k_1} - i)h] - \boldsymbol{y}[(s^{\boldsymbol{y}}_{k_1} - i)h], & t \in \mathcal{B}_1,\\ \boldsymbol{y}[(s^{\boldsymbol{y}}_{k_1} - i)h] - \boldsymbol{y}[(s^{\boldsymbol{y}}_{k_1} - i)h + h], & t \in \mathcal{B}_2,\\ \quad\vdots & \quad\vdots\\ \boldsymbol{y}[(s^{\boldsymbol{y}}_{k_1} - i)h] - \boldsymbol{y}[(s^{\boldsymbol{y}}_{k_1} - i)h + (\phi_{k_1} - 1)h], & t \in \mathcal{B}_{\phi_{k_1}}, \end{cases} \tag{10}$$

where $\delta_{2_j}(t)$ is obtained from Eq. (9) by replacing $s^{\boldsymbol{y}}_{k_1}$ with $s^{\boldsymbol{u}}_{k_2}$. $\boldsymbol{e}_{2_j}(t)$ is obtained from Eq. (10) by replacing $s^{\boldsymbol{y}}_{k_1}$ with $s^{\boldsymbol{u}}_{k_2}$ and $\boldsymbol{y}$ with $\bar{\boldsymbol{u}}$.

Based on the definitions of $\delta_{1_i}(t)$ and $\delta_{2_j}(t)$, the following deductions can be made:

$$\begin{aligned}
&\underline{\delta}_{1_i} \triangleq ih \leq \delta_{1_i}(t) \leq (i+1)h + \tau_{1_{\mathrm{M}}} \triangleq \overline{\delta}_{1_i},\\
&\underline{\delta}_{2_j} \triangleq jh \leq \delta_{2_j}(t) \leq (j+1)h + \tau_{2_{\mathrm{M}}} \triangleq \overline{\delta}_{2_j}.
\end{aligned}$$

Then, based on Eqs. (9) and (10), the equations hold as follows:

$$\begin{aligned}
&\boldsymbol{y}(s^{\boldsymbol{y}}_{k_1} h - ih) = \boldsymbol{e}_{1_i}(t) + \boldsymbol{y}(t - \delta_{1_i}(t)),\ t \in [t^{\boldsymbol{y}}_{k_1}, t^{\boldsymbol{y}}_{k_1+1}),\\
&\bar{\boldsymbol{u}}(s^{\boldsymbol{u}}_{k_2} h - jh) = \boldsymbol{e}_{2_j}(t) + \bar{\boldsymbol{u}}(t - \delta_{2_j}(t)), t \in [t^{\boldsymbol{u}}_{k_2}, t^{\boldsymbol{u}}_{k_2+1}).
\end{aligned}$$

Remark 2 With the above analysis, the discrete inputs of the DOFC and the error system could be represented in continuous form as $\tilde{\boldsymbol{y}}(t) = \boldsymbol{y}_{\mathrm{d}}(s^{\boldsymbol{y}}_{k_1} h)$, $t \in [t^{\boldsymbol{y}}_{k_1}, t^{\boldsymbol{y}}_{k_1+1})$, and $\boldsymbol{u}(t, r_t, q_t) = \bar{\boldsymbol{u}}(s^{\boldsymbol{u}}_{k_2} h) = \boldsymbol{e}_{2_0}(t) + \bar{\boldsymbol{u}}(t - \delta_{2_0}(t))$, $t \in [t^{\boldsymbol{u}}_{k_2}, t^{\boldsymbol{u}}_{k_2+1})$, respectively. Yue et al. (2013) first introduced the concept of transforming discrete signals into continuous ones. This concept was subsequently refined in Zhang XM and Han (2014). Motivated by these findings, we formulate a series of functions in Eqs. (9) and (10) to manage the discrete signals within the framework of our proposed SDDETM.

Subsequently, we introduce the T–S fuzzy DOFC.

Control Rule m: if $\theta_1(t^{\boldsymbol{y}}_{k_1})$ denotes υ^m_1, $\cdots$, $\theta_k(t^{\boldsymbol{y}}_{k_1})$ denotes υ^m_k, then

$$\begin{cases} \dot{\boldsymbol{x}}_{\mathrm{c}}(t) = \boldsymbol{A}_{km}\boldsymbol{x}_{\mathrm{c}}(t) + \boldsymbol{B}_{km}\boldsymbol{x}_{\mathrm{c}}(t - \delta_{1_0}(t))\\ \qquad\qquad + \boldsymbol{C}_{km}\boldsymbol{x}_{\mathrm{c}}(t - \delta_{2_0}(t)) + \boldsymbol{D}_{km}\tilde{\boldsymbol{y}}(t),\\ \bar{\boldsymbol{u}}(t) = \boldsymbol{F}_{km}\boldsymbol{x}_{\mathrm{c}}(t). \end{cases} \tag{11}$$

Here, $\boldsymbol{x}_c(t) \in \mathbb{R}^a$ is the DOFC's internal state, and $\boldsymbol{A}_{km}$, $\boldsymbol{B}_{km}$, $\boldsymbol{C}_{km}$, $\boldsymbol{D}_{km}$, and $\boldsymbol{F}_{km}$ are the controller matrices. Hence, the associated fuzzy DOFC can be expressed as follows:

$$\begin{cases} \dot{\boldsymbol{x}}_{\mathrm{c}}(t) = \sum_{m=1}^{L} h_m(\boldsymbol{\theta}(t^{\boldsymbol{y}}_{k_1}))[\boldsymbol{A}_{km}\boldsymbol{x}_{\mathrm{c}}(t)\\ \qquad\qquad + \boldsymbol{B}_{km}\boldsymbol{x}_{\mathrm{c}}(t - \delta_{1_0}(t)) + \boldsymbol{C}_{km}\boldsymbol{x}_{\mathrm{c}}(t - \delta_{2_0}(t))\\ \qquad\qquad + \boldsymbol{D}_{km}\tilde{\boldsymbol{y}}(t)],\\ \bar{\boldsymbol{u}}(t) = \sum_{m=1}^{L} h_m(\boldsymbol{\theta}(t^{\boldsymbol{y}}_{k_1}))\boldsymbol{F}_{km}\boldsymbol{x}_{\mathrm{c}}(t), \end{cases} \tag{12}$$

where $h_m(\boldsymbol{\theta}(t^{\boldsymbol{y}}_{k_1})) = \frac{\lambda_m(\boldsymbol{\theta}(t^{\boldsymbol{y}}_{k_1}))}{\sum_{d=1}^{L}\lambda_d(\boldsymbol{\theta}(t^{\boldsymbol{y}}_{k_1}))}$, $h_m(\boldsymbol{\theta}(t^{\boldsymbol{y}}_{k_1})) \in [0, 1]$, $\sum_{m=1}^{L} h_m(\boldsymbol{\theta}(t^{\boldsymbol{y}}_{k_1})) = 1$, $\lambda_m(\boldsymbol{\theta}(t^{\boldsymbol{y}}_{k_1})) = \mathit{\Pi}_{d=1}^{k}\varrho^m_d(\boldsymbol{\theta}(t^{\boldsymbol{y}}_{k_1}))$, and $\varrho^m_d(\boldsymbol{\theta}(t^{\boldsymbol{y}}_{k_1}))$ is the grade membership of $\boldsymbol{\theta}(t^{\boldsymbol{y}}_{k_1})$ in υ^m_d.

Assumption 4 Assume that there is no direct relationship between system delay and transmission delay during the data transmission process in the closed-loop system.

2.5 Design objective

To simplify the formulations, let $h_l = h_l(\boldsymbol{\theta}(t))$, $h_m = h_m(\boldsymbol{\theta}(t^{\boldsymbol{y}}_{k_1}))$, $l, m \in \mathcal{N}_L$, $b^{\mathrm{s}}(r_t) = b^{\mathrm{s}}$, $b^{\mathrm{c}}(q_t) = b^{\mathrm{c}}$, $1 - b^{\mathrm{s}}(r_t) = \bar{b}^{\mathrm{s}}$, and $1 - b^{\mathrm{c}}(q_t) = \bar{b}^{\mathrm{c}}$. From

Eqs. (3) and (12), for $t \in \mathcal{I}_{\rm c} = [t^{\boldsymbol{y}}_{k_1}, t^{\boldsymbol{y}}_{k_1+1}) \cup [t^{\boldsymbol{u}}_{k_2}, t^{\boldsymbol{u}}_{k_2+1})$, the augmented closed-loop system is formulated as follows:

$$\begin{aligned}\dot{\boldsymbol{x}}(t) = &\sum_{l=1}^{L}\sum_{m=1}^{L} h_l h_m[\boldsymbol{A}^0_{lm}\boldsymbol{x}(t) + \boldsymbol{A}^1_{lm}\boldsymbol{x}(t-\delta_{1_0}(t))\\ &+ \boldsymbol{A}^2_{lm}\boldsymbol{x}(t-\delta_{2_0}(t)) + \boldsymbol{A}^3_{m}\boldsymbol{e}_{1_0}(t) + \boldsymbol{A}^4_{l}\boldsymbol{e}_{2_0}(t)\\ &+ \boldsymbol{A}^5_{l}\boldsymbol{\varphi}_1(\boldsymbol{x}(t)) + \boldsymbol{A}^6_{l}\boldsymbol{\varphi}_2(\boldsymbol{x}(t-h(t)))\\ &+ \boldsymbol{A}^7_{m}\boldsymbol{\mathscr{G}}_{\rm s}(\boldsymbol{y}(t^{\boldsymbol{y}}_{k_1})) + \boldsymbol{A}^8_{l}\boldsymbol{\mathscr{G}}_{\rm c}(\bar{\boldsymbol{u}}(t^{\boldsymbol{u}}_{k_2}))],\end{aligned} \tag{13}$$

where $\boldsymbol{x}(t) = \mathrm{col}\{\boldsymbol{x}_{\rm e}(t),\ \boldsymbol{x}_{\rm c}(t)\}$,

$$\boldsymbol{A}^0_{lm} = \begin{bmatrix}\boldsymbol{A}_l & \boldsymbol{0}\\ \boldsymbol{0} & \boldsymbol{A}_{km}\end{bmatrix}, \boldsymbol{A}^1_{lm} = \begin{bmatrix}\boldsymbol{0} & \boldsymbol{0}\\ b^{\rm s}\boldsymbol{D}_{km}\boldsymbol{D}_l & \boldsymbol{B}_{km}\end{bmatrix},$$
$$\boldsymbol{A}^2_{lm} = \begin{bmatrix}\boldsymbol{0} & b^{\rm s}\boldsymbol{E}_l\boldsymbol{F}_{km}\\ \boldsymbol{0} & \boldsymbol{C}_{km}\end{bmatrix}, \boldsymbol{A}^3_{m} = \begin{bmatrix}\boldsymbol{0}\\ b^{\rm s}\boldsymbol{D}_{km}\end{bmatrix},$$
$$\boldsymbol{A}^4_{l} = \begin{bmatrix}b^{\rm c}\boldsymbol{E}_l\\ \boldsymbol{0}\end{bmatrix}, \boldsymbol{A}^5_{l} = \begin{bmatrix}\boldsymbol{B}_l & \boldsymbol{0}\\ \boldsymbol{0} & \boldsymbol{0}\end{bmatrix}, \boldsymbol{A}^6_{l} = \begin{bmatrix}\boldsymbol{C}_l & \boldsymbol{0}\\ \boldsymbol{0} & \boldsymbol{0}\end{bmatrix},$$
$$\boldsymbol{A}^7_{m} = \begin{bmatrix}\boldsymbol{0}\\ \bar{b}^{\rm s}\boldsymbol{D}_{km}\end{bmatrix}, \boldsymbol{A}^8_{l} = \begin{bmatrix}\bar{b}^{\rm c}\boldsymbol{E}_l\\ \boldsymbol{0}\end{bmatrix}.$$

Similar to Tan et al. (2020), to account for asynchronous premise variables, we assume the presence of $\alpha_m > 0$ and $\nu_m > 0$, provided that the following expressions hold:

$$\begin{aligned}&|h_m(\boldsymbol{\theta}(t^{\boldsymbol{y}}_{k1}) - h_m(\boldsymbol{\theta}(t))| \le \nu_m,\\ &h_m(\boldsymbol{\theta}(t^{\boldsymbol{y}}_{k1})) = \alpha_m h_m(\boldsymbol{\theta}(t)).\end{aligned}$$

It is obvious that $\gamma^m_1 = 1 - \frac{\nu_m}{h_l(\boldsymbol{\theta}(t))} \le \alpha_m \le 1 + \frac{\nu_m}{h_l(\boldsymbol{\theta}(t))} = \gamma^m_2$. Therefore,

$$\begin{aligned}\zeta_1 =& \frac{\min\{\gamma^m_1\}}{\max\{\gamma^m_2\}} \le \frac{\min\{\alpha_l\}}{\max\{\alpha_m\}} \le \frac{\alpha_l}{\alpha_m}\\ &\le \frac{\max\{\alpha_l\}}{\min\{\alpha_m\}} \le \frac{\min\{\gamma^m_1\}}{\max\{\gamma^m_2\}} = \zeta_2.\end{aligned} \tag{14}$$

The augmented closed-loop system (13) is represented as below:

$$\begin{aligned}\dot{\boldsymbol{x}}(t) = &\sum_{l=1}^{L}\sum_{m=1}^{L} \alpha_m h_l h_m[\boldsymbol{A}^0_{lm}\boldsymbol{x}(t) + \boldsymbol{A}^1_{lm}\boldsymbol{x}(t-\delta_{1_0}(t))\\ &+ \boldsymbol{A}^2_{lm}\boldsymbol{x}(t-\delta_{2_0}(t)) + \boldsymbol{A}^3_{lm}\boldsymbol{e}_{1_0}(t) + \boldsymbol{A}^4_{l}\boldsymbol{e}_{2_0}(t)\\ &+ \boldsymbol{A}^5_{l}\boldsymbol{\varphi}_1(\boldsymbol{x}(t)) + \boldsymbol{A}^6_{l}\boldsymbol{\varphi}_2(\boldsymbol{x}(t-h(t)))\\ &+ \boldsymbol{A}^7_{m}\boldsymbol{\mathscr{G}}_{\rm s}(\boldsymbol{y}(t^{\boldsymbol{y}}_{k_1})) + \boldsymbol{A}^8_{l}\boldsymbol{\mathscr{G}}_{\rm c}(\bar{\boldsymbol{u}}(t^{\boldsymbol{u}}_{k_2}))].\end{aligned} \tag{15}$$

The primary objective of this study is to concurrently optimize the parameters of the DOFC in Eq. (12) and the SDDETM $\boldsymbol{\Phi}_{1_i}, \boldsymbol{\Phi}_{2_j}$ in Eqs. (4) and (5) to make the closed-loop system (15) asymptotically stable, thereby minimizing unnecessary consumption. This involves ensuring system stability under deception attacks and efficient use of network resources through the SDDETM.

3 Main results

In this section, the stability criteria for the closed-loop system (15) are established in Theorem 1. The sufficient conditions for obtaining stabilizing DOFC and SDDETM parameters are presented in Proposition 1 and Theorem 2.

Theorem 1 For $i \in \mathcal{N}_{N_1}$, $j \in \mathcal{N}_{N_2}$, $\mathscr{B} \in \{1,2\}$, $\mathscr{C} \in \{3,4\}$, given positive scalars $\underline{\delta}_{1_i}$, $\overline{\delta}_{1_i}$, $\underline{\delta}_{2_j}$, $\overline{\delta}_{2_j}$, ϵ_{1_i}, ϵ_{2_j}, $N_{\mathscr{B}}$, $w_{\mathscr{B}}$, $\mu_{\mathscr{B}}$, $\zeta_{\mathscr{B}}$, and the diagonal matrices $\mathscr{K}_{\rm m}$, $\mathscr{K}_{\rm M}$, and real matrices $\boldsymbol{G}_{\rm s}$, $\boldsymbol{G}_{\rm c}$, the closed-loop system (15) is asymptotically stable with the proposed SDDETM if there exist positive diagonal matrices $\boldsymbol{T}_1$ and $\boldsymbol{T}_2$, $\boldsymbol{P}$, $\boldsymbol{P}_{\mathscr{B}_i}$, $\boldsymbol{P}_{\mathscr{C}_j}$, $\boldsymbol{P}_5 \in \mathcal{S}^+_n$, $\boldsymbol{\Phi}_{1_i} \in \mathcal{S}^+_c$, $\boldsymbol{\Phi}_{2_j} \in \mathcal{S}^+_b$, and matrices $\boldsymbol{X}_{1_i}$, $\boldsymbol{X}_{2_j}$, and $\boldsymbol{X}_3$ such that the following inequalities hold:

$$\boldsymbol{\Theta}^{11}_l = \begin{bmatrix}\boldsymbol{\Pi}^{11}_{ll} & *\\ \boldsymbol{\Pi}^{12}_{ll} & \boldsymbol{\Pi}_{13}\end{bmatrix} < 0, \tag{16}$$

$$\boldsymbol{\Theta}^{12}_{lm} = \begin{bmatrix}\boldsymbol{\Pi}^{11}_{lm} + \zeta_1\boldsymbol{\Pi}^{11}_{ml} & * & *\\ \boldsymbol{\Pi}^{12}_{lm} & \boldsymbol{\Pi}_{13} & *\\ \zeta_2\boldsymbol{\Pi}^{12}_{ml} & \boldsymbol{0} & \zeta_2\boldsymbol{\Pi}_{13}\end{bmatrix} < 0, \tag{17}$$

$$\boldsymbol{\Theta}^{13}_{lm} = \begin{bmatrix}\boldsymbol{\Pi}^{11}_{lm} + \zeta_2\boldsymbol{\Pi}^{11}_{ml} & * & *\\ \boldsymbol{\Pi}^{12}_{lm} & \boldsymbol{\Pi}_{13} & *\\ \zeta_2\boldsymbol{\Pi}^{12}_{ml} & \boldsymbol{0} & \zeta_2\boldsymbol{\Pi}_{13}\end{bmatrix} < 0, \tag{18}$$

$$\begin{bmatrix}\boldsymbol{P}_{2_i} & \boldsymbol{X}_{1_i}\\ * & \boldsymbol{P}_{2_i}\end{bmatrix} \ge 0, \begin{bmatrix}\boldsymbol{P}_{4_j} & \boldsymbol{X}_{2_j}\\ * & \boldsymbol{P}_{4_j}\end{bmatrix} \ge 0, \begin{bmatrix}\boldsymbol{P}_5 & \boldsymbol{X}_3\\ * & \boldsymbol{P}_5\end{bmatrix} \ge 0,$$

where

$$\boldsymbol{\Pi}^{11}_{lm} = \begin{bmatrix}\boldsymbol{\beta}^{11}_{lm} & \boldsymbol{\beta}^{12}_{lm} & \boldsymbol{\beta}^{13}_{lm} & \boldsymbol{\beta}^{14}_{l} & \boldsymbol{0} & \boldsymbol{P}\boldsymbol{A}^7_m & \boldsymbol{P}\boldsymbol{A}^8_l\\ * & \boldsymbol{\beta}^{22} & \boldsymbol{0} & \beta^{24} & \boldsymbol{0} & \boldsymbol{0} & \boldsymbol{0}\\ * & * & \boldsymbol{\beta}^{33} & \boldsymbol{0} & \boldsymbol{0} & \boldsymbol{0} & \boldsymbol{0}\\ * & * & * & \boldsymbol{\beta}^{44} & \boldsymbol{0} & \boldsymbol{0} & \boldsymbol{0}\\ * & * & * & * & \boldsymbol{\beta}^{55} & \boldsymbol{0} & \boldsymbol{0}\\ * & * & * & * & * & -w_1\boldsymbol{I} & \boldsymbol{0}\\ * & * & * & * & * & * & -w_2\boldsymbol{I}\end{bmatrix}.$$

Here, $\boldsymbol{\beta}^{11}_{lm} = \mathrm{He}(\boldsymbol{P}\boldsymbol{A}^0_{lm}) - \sum_{i=0}^{N_1}\boldsymbol{P}_{1i} - \sum_{j=0}^{N_2}\boldsymbol{P}_{3j} - \boldsymbol{P}_5 - 2\boldsymbol{E}^{\rm T}_1\mathscr{K}^{\rm T}_{\rm m}\boldsymbol{T}_1\mathscr{K}_{\rm M}\boldsymbol{E}_1$, $\boldsymbol{E}_1 = [\boldsymbol{I}_n\ \boldsymbol{0}_n]$

and $\boldsymbol{E}_2=[\boldsymbol{0}_n\ \boldsymbol{I}_n]$.

$$
\begin{aligned}
\boldsymbol{\beta}_{lm}^{12}=&[\boldsymbol{P}\boldsymbol{\mathcal{A}}_{lm}^1+[\boldsymbol{\vartheta}_{lm}^{10}\ \boldsymbol{\vartheta}_{lm}^{11}\ \cdots\ \boldsymbol{\vartheta}_{lm}^{1N_1}],\\
&\boldsymbol{P}\boldsymbol{\mathcal{A}}_{lm}^2+[\boldsymbol{\vartheta}_{lm}^{20}\ \boldsymbol{\vartheta}_{lm}^{21}\ \cdots\ \boldsymbol{\vartheta}_{lm}^{2N_2}],\boldsymbol{P}_5-\boldsymbol{X}_3^{\mathrm{T}},\ \boldsymbol{X}_3^{\mathrm{T}}],\\
\boldsymbol{\vartheta}_{lm}^{1i}=&[\boldsymbol{P}_{1i}\ \boldsymbol{0}_{n,2n}],\\
\boldsymbol{\vartheta}_{lm}^{2j}=&[\boldsymbol{P}_{3j}\ \boldsymbol{0}_{n,2n}],\\
\boldsymbol{\mathcal{A}}_{lm}^1=&[\boldsymbol{0}_n,\ \boldsymbol{A}_{lm}^1,\ \boldsymbol{0}_{n,(3N_1+1)n}],\\
\boldsymbol{\mathcal{A}}_{lm}^2=&[\boldsymbol{0}_n,\ \boldsymbol{A}_{lm}^2,\ \boldsymbol{0}_{n,(3N_2+1)n}],\\
\boldsymbol{\beta}_{lm}^{13}=&\boldsymbol{P}[\boldsymbol{\mathcal{A}}_m^3\ \boldsymbol{\mathcal{A}}_l^4],\\
\boldsymbol{\beta}_l^{14}=&[\boldsymbol{P}\boldsymbol{A}_l^5+\boldsymbol{E}_1^{\mathrm{T}}\boldsymbol{T}_1(k_{\mathrm{m}}+k_{\mathrm{M}})\ \boldsymbol{P}\boldsymbol{A}_l^6],\\
\boldsymbol{\mathcal{A}}_m^3=&[\boldsymbol{A}_m^3\ \boldsymbol{0}_{n,N_1c}],\ \boldsymbol{\mathcal{A}}_l^4=[\boldsymbol{A}_l^4\ \boldsymbol{0}_{n,N_2b}],\\
\boldsymbol{\beta}^{22}=&\mathrm{diag}\{\boldsymbol{M}_{10},\boldsymbol{M}_{11},\cdots,\boldsymbol{M}_{1N_1},\\
&\boldsymbol{M}_{20},\boldsymbol{M}_{21},\cdots,\boldsymbol{M}_{2N_2},\boldsymbol{M}_3\},\\
\boldsymbol{M}_{1i}=&\begin{bmatrix}-\boldsymbol{P}_{1i}-\boldsymbol{P}_{2i} & \boldsymbol{P}_{2i}-\boldsymbol{X}_{1i}^{\mathrm{T}} & \boldsymbol{X}_{1i}^{\mathrm{T}}\\ * & -2\boldsymbol{P}_{2i}+\mathrm{He}(\boldsymbol{X}_{1i}) & \boldsymbol{P}_{2i}-\boldsymbol{X}_{1i}^{\mathrm{T}}\\ * & * & -\boldsymbol{P}_{2i}\end{bmatrix},\\
\boldsymbol{M}_{2j}=&\begin{bmatrix}-\boldsymbol{P}_{3j}-\boldsymbol{P}_{4j} & \boldsymbol{P}_{4j}-\boldsymbol{X}_{2j}^{\mathrm{T}} & \boldsymbol{X}_{2j}^{\mathrm{T}}\\ * & -2\boldsymbol{P}_{4j}+\mathrm{He}(X_{2j}) & \boldsymbol{P}_{4j}-\boldsymbol{X}_{2j}^{\mathrm{T}}\\ * & * & -\boldsymbol{P}_{4j}\end{bmatrix},\\
\boldsymbol{M}_3=&\begin{bmatrix}-2\boldsymbol{P}_5+\mathrm{He}(\boldsymbol{X}_3) & -2\boldsymbol{E}_1^{\mathrm{T}}\mathscr{K}_{\mathrm{m}}^{\mathrm{T}}\boldsymbol{T}_2\mathscr{K}_{\mathrm{M}}\boldsymbol{E}_1\ \boldsymbol{P}_5-\boldsymbol{X}_3^{\mathrm{T}}\\ * & -\boldsymbol{P}_5\end{bmatrix},\\
\boldsymbol{\beta}^{33}=&-\mathrm{diag}\{\boldsymbol{\Phi}_{10},\boldsymbol{\Phi}_{11},\cdots,\boldsymbol{\Phi}_{1N_1},\\
&\boldsymbol{\Phi}_{20},\boldsymbol{\Phi}_{21},\cdots,\boldsymbol{\Phi}_{2N_2}\},\\
\boldsymbol{\beta}^{24}=&\begin{bmatrix}\boldsymbol{0}_{3(N_1+N_2+2)n,a} & \boldsymbol{0}_{3(N_1+N_2+2)n,a}\\ \boldsymbol{0}_{2n,a} & [(\mathscr{K}_{\mathrm{m}}+\mathscr{K}_{\mathrm{M}})^{\mathrm{T}}\boldsymbol{T}_2^{\mathrm{T}}\boldsymbol{E}_1^{\mathrm{T}}\ \boldsymbol{0}_{a,n}]^{\mathrm{T}}\end{bmatrix},\\
\boldsymbol{\beta}^{44}=&\mathrm{diag}\{-2\boldsymbol{T}_1,-2\boldsymbol{T}_2\},\ \boldsymbol{\beta}^{55}=\mathrm{diag}\{-\mu_1\boldsymbol{I},-\mu_2\boldsymbol{I}\},\\
\boldsymbol{\Pi}_{lm}^{12}=&[(\boldsymbol{F}_{lm}^1)^{\mathrm{T}}\boldsymbol{\mathcal{D}}\ \ (\boldsymbol{F}_{lm}^2)^{\mathrm{T}}\ \ (\boldsymbol{F}_l^3)^{\mathrm{T}}\ \ (\boldsymbol{F}_m^4)^{\mathrm{T}}]^{\mathrm{T}},\\
\boldsymbol{F}_{lm}^1=&[\boldsymbol{A}_{lm}^0\ \boldsymbol{\mathcal{A}}_{lm}^1\ \boldsymbol{\mathcal{A}}_{lm}^2\ \boldsymbol{0}_{n,2n}\ \boldsymbol{\mathcal{A}}_m^3\ \boldsymbol{\mathcal{A}}_l^4\ \boldsymbol{A}_l^5\ \boldsymbol{A}_l^6\\
&\boldsymbol{0}_{n,2}\ \boldsymbol{A}_m^7\ \boldsymbol{A}_l^8],\\
\boldsymbol{\mathcal{D}}=&[\underline{\delta}_{1_0},\cdots,\underline{\delta}_{1N_1},(\overline{\delta}_{1_0},-\underline{\delta}_{1_0}),\cdots,(\overline{\delta}_{1N_1},-\underline{\delta}_{1N_1}),\\
&\underline{\delta}_{2_0},\cdots,\underline{\delta}_{2N_2},(\overline{\delta}_{2_0},-\underline{\delta}_{2_0}),\cdots,(\overline{\delta}_{2N_2},-\underline{\delta}_{2N_2}),\\
&h_{\mathrm{M}}],\\
\boldsymbol{F}_{lm}^2=&\mathrm{col}\{\boldsymbol{H}_{10},\ \boldsymbol{H}_{11},\ \cdots,\ \boldsymbol{H}_{1N_1},\ \boldsymbol{H}_{20},\\
&\boldsymbol{H}_{21},\ \cdots,\ \boldsymbol{H}_{2N_2}\},\\
\boldsymbol{H}_{1i}=&[\boldsymbol{0}_{c,(3i-1)n}\ \boldsymbol{D}_l\boldsymbol{E}_1\ \boldsymbol{0}_{c,[3(N_1+N_2-i)+10]n+N}],\\
&i\in\mathcal{N}_{N_1},\\
\boldsymbol{H}_{2j}=&[\boldsymbol{0}_{b,[3(N_1+j)+2]n}\ \boldsymbol{F}_{km}\boldsymbol{E}_2\ \boldsymbol{0}_{b,[3(N_2-j)+7]n+N}],\\
&j\in\mathcal{N}_{N_2},\\
\boldsymbol{F}_l^3=&[\boldsymbol{0}_{c,2n}\ \boldsymbol{G}_{\mathrm{s}}\boldsymbol{D}_l\boldsymbol{E}_1\ \boldsymbol{0}_{c,[3(N_1+N_2)+6]n}\ \boldsymbol{G}_{\mathrm{s}}\ \boldsymbol{0}_{c,N+n-c}],\\
\boldsymbol{F}_m^4=&[\boldsymbol{0}_{b,(3N_1+5)n}\ \boldsymbol{G}_{\mathrm{c}}\boldsymbol{F}_{km}\boldsymbol{E}_2\ \boldsymbol{0}_{b,(3N_2+3)n+(N_1+1)c}\\
&\boldsymbol{G}_{\mathrm{c}}\ \boldsymbol{0}_{b,(N_2+1)b+n+c+2}],\\
N=&(N_1+2)c+(N_2+2)b+2,\\
\boldsymbol{\Pi}_{13}=&\mathrm{diag}\{\boldsymbol{\mathcal{E}},(\boldsymbol{\Delta}\boldsymbol{\beta}^{33})^{-1},-\boldsymbol{I},-\boldsymbol{I}\},
\end{aligned}
$$

$$
\begin{aligned}
\boldsymbol{\mathcal{E}}=&-\mathrm{diag}\{\boldsymbol{P}_{10}^{-1},\cdots,\boldsymbol{P}_{1N_1}^{-1},\boldsymbol{P}_{20}^{-1},\cdots,\boldsymbol{P}_{2N_1}^{-1},\\
&\boldsymbol{P}_{30}^{-1},\cdots,\boldsymbol{P}_{3N_2}^{-1},\boldsymbol{P}_{40}^{-1},\cdots,\boldsymbol{P}_{4N_2}^{-1},\boldsymbol{P}_5^{-1}\},\\
\boldsymbol{\Delta}=&\mathrm{diag}\{\epsilon_{1_0},\epsilon_{1_1},\cdots,\epsilon_{1_{N_1}},\epsilon_{2_0},\epsilon_{2_1},\cdots,\epsilon_{2_{N_2}}\}.
\end{aligned}
$$

Proof Choose a Lyapunov functional candidate as follows:

$$
V(t)=V_1(t)+\sum_{i=0}^{N_1}V_2^i(t)+\sum_{j=0}^{N_2}V_3^j(t)+V_4(t),\quad(19)
$$

where

$$
\begin{aligned}
V_1(t)=&\boldsymbol{x}^{\mathrm{T}}(t)\boldsymbol{P}\boldsymbol{x}(t)+\eta_1(t)+\eta_2(t),\\
V_2^i(t)=&\underline{\delta}_{1_i}\int_{-\underline{\delta}_{1_i}}^0\int_{t+\theta}^t\dot{\boldsymbol{x}}^{\mathrm{T}}(s)\boldsymbol{P}_{1_i}\dot{\boldsymbol{x}}(s)\mathrm{d}s\mathrm{d}\theta\\
&+(\overline{\delta}_{1_i}-\underline{\delta}_{1_i})\int_{-\overline{\delta}_{1_i}}^{-\underline{\delta}_{1_i}}\int_{t+\theta}^t\dot{\boldsymbol{x}}^{\mathrm{T}}(s)\boldsymbol{P}_{2_i}\dot{\boldsymbol{x}}(s)\mathrm{d}s\mathrm{d}\theta,\\
V_3^j(t)=&\underline{\delta}_{2_j}\int_{-\underline{\delta}_{2_j}}^0\int_{t+\theta}^t\dot{\boldsymbol{x}}^{\mathrm{T}}(s)\boldsymbol{P}_{3_j}\dot{\boldsymbol{x}}(s)\mathrm{d}s\mathrm{d}\theta\\
&+(\overline{\delta}_{2_j}-\underline{\delta}_{2_j})\int_{-\overline{\delta}_{2_j}}^{-\underline{\delta}_{2_j}}\int_{t+\theta}^t\dot{\boldsymbol{x}}^{\mathrm{T}}(s)\boldsymbol{P}_{4_j}\dot{\boldsymbol{x}}(s)\mathrm{d}s\mathrm{d}\theta,\\
V_4(t)=&h_{\mathrm{M}}\int_{-h_{\mathrm{M}}}^0\int_{t+\theta}^t\dot{\boldsymbol{x}}^{\mathrm{T}}(s)\boldsymbol{P}_5\dot{\boldsymbol{x}}(s)\mathrm{d}s\mathrm{d}\theta.
\end{aligned}\quad(20)
$$

From Eqs. (6) and (7), for $t\in\mathcal{I}_{\mathrm{c}}$, we have

$$
\begin{aligned}
\boldsymbol{\mathcal{A}}_3=&\boldsymbol{y}^{\mathrm{T}}(t)w_1\boldsymbol{G}_{\mathrm{s}}^{\mathrm{T}}\boldsymbol{G}_{\mathrm{s}}\boldsymbol{y}(t)-w_1\boldsymbol{\mathscr{G}}_{\mathrm{s}}^{\mathrm{T}}(\boldsymbol{y}(t))\boldsymbol{\mathscr{G}}_{\mathrm{s}}(\boldsymbol{y}(t))\geq0,\\
\boldsymbol{\mathcal{A}}_4=&\bar{\boldsymbol{u}}^{\mathrm{T}}(t)w_2\boldsymbol{G}_{\mathrm{c}}^{\mathrm{T}}\boldsymbol{G}_{\mathrm{c}}\bar{\boldsymbol{u}}(t)-w_2\boldsymbol{\mathscr{G}}_{\mathrm{c}}(\bar{\boldsymbol{u}}(t))\boldsymbol{\mathscr{G}}_{\mathrm{c}}^{\mathrm{T}}(\bar{\boldsymbol{u}}(t))\geq0.
\end{aligned}
$$

Thus, the time derivative of $V_k(t)$ $(k\in\mathcal{N}_{4+})$ satisfies

$$
\begin{aligned}
&\mathbb{E}\{\dot{V}(t)\}\\
\leq&\sum_{l=1}^L\sum_{m=1}^L2\alpha_mh_lh_m\mathbb{E}\{\boldsymbol{x}^{\mathrm{T}}(t)\boldsymbol{P}\dot{\boldsymbol{x}}(t)\}+\boldsymbol{\mathcal{A}}_3\\
&+\boldsymbol{\mathcal{A}}_4+\mathbb{E}\{\dot{\boldsymbol{x}}^{\mathrm{T}}(t)\boldsymbol{\mathcal{F}}\dot{\boldsymbol{x}}(t)\}+\dot{\eta}_1+\dot{\eta}_2\\
&-\sum_{i=0}^{N_1}\Bigg[\underline{\delta}_{1_i}\int_{t-\underline{\delta}_{1_i}}^t\dot{\boldsymbol{x}}^{\mathrm{T}}(s)\boldsymbol{P}_{1_i}\dot{\boldsymbol{x}}(s)\mathrm{d}s\\
&+(\overline{\delta}_{1_i}-\underline{\delta}_{1_i})\int_{t-\overline{\delta}_{1_i}}^{t-\underline{\delta}_{1_i}}\dot{\boldsymbol{x}}^{\mathrm{T}}(s)\boldsymbol{P}_{2_i}\dot{\boldsymbol{x}}(s)\mathrm{d}s\Bigg]\\
&-\sum_{j=0}^{N_2}\Bigg[\underline{\delta}_{2_j}\int_{t-\underline{\delta}_{2_j}}^t\dot{\boldsymbol{x}}^{\mathrm{T}}(s)\boldsymbol{P}_{3_j}\dot{\boldsymbol{x}}(s)\mathrm{d}s\\
&-(\overline{\delta}_{2_j}-\underline{\delta}_{2_j})\int_{t-\overline{\delta}_{2_j}}^{t-\underline{\delta}_{2_j}}\dot{\boldsymbol{x}}^{\mathrm{T}}(s)\boldsymbol{P}_{4_j}\dot{\boldsymbol{x}}(s)\mathrm{d}s\Bigg]\\
&-h_{\mathrm{M}}\int_{t-h_{\mathrm{M}}}^t\dot{\boldsymbol{x}}^{\mathrm{T}}(s)\boldsymbol{P}_5\dot{\boldsymbol{x}}(s)\mathrm{d}s,
\end{aligned}\quad(21)
$$

where $\boldsymbol{\mathcal{F}}=\sum_{i=0}^{N_1}[\underline{\delta}_{1_i}^2\boldsymbol{P}_{1_i}+(\overline{\delta}_{1_i}-\underline{\delta}_{1_i})^2\boldsymbol{P}_{2_i}]+h_{\mathrm{M}}^2\boldsymbol{G}_5+\sum_{j=0}^{N_2}[\underline{\delta}_{2_j}^2\boldsymbol{P}_{3_j}+(\overline{\delta}_{2_j}-\underline{\delta}_{2_j})^2\boldsymbol{P}_{4_j}]$. From Jensen's inequality (Boyd et al., 1994), it follows that

$$\begin{aligned}
&-\underline{\delta}_{1_i}\int_{t-\underline{\delta}_{1_i}}^{t}\dot{\boldsymbol{x}}^{\mathrm{T}}(s)\boldsymbol{P}_{1_i}\dot{\boldsymbol{x}}(s)\mathrm{d}s\\
\le&-[*]^{\mathrm{T}}\boldsymbol{P}_{1_i}[\boldsymbol{x}(t)-\boldsymbol{x}(t-\underline{\delta}_{1_i})],\\
&-\underline{\delta}_{2_j}\int_{t-\underline{\delta}_{2_j}}^{t}\dot{\boldsymbol{x}}^{\mathrm{T}}(s)\boldsymbol{P}_{3_j}\dot{\boldsymbol{x}}(s)\mathrm{d}s\\
\le&-[*]^{\mathrm{T}}\boldsymbol{P}_{3_j}[\boldsymbol{x}(t)-\boldsymbol{x}(t-\underline{\delta}_{2_j})].
\end{aligned}$$

Subsequently, using Lemma 3 in Zhang LR et al. (2020), the integral terms in Eq. (19) can be relaxed as

$$\begin{aligned}
&(\underline{\delta}_{1_i}-\overline{\delta}_{1_i})\int_{t-\overline{\delta}_{1_i}}^{t-\underline{\delta}_{1_i}}\dot{\boldsymbol{x}}^{\mathrm{T}}(s)\boldsymbol{P}_{2_i}\dot{\boldsymbol{x}}(s)\mathrm{d}s\\
\le&[*]\boldsymbol{\mathcal{M}}_1^i\begin{bmatrix}\boldsymbol{x}(t-\underline{\delta}_{1_i})\\ \boldsymbol{x}(t-\delta_{1_i}(t))\\ \boldsymbol{x}(t-\overline{\delta}_{1_i})\end{bmatrix},\\
&(\underline{\delta}_{2_j}-\overline{\delta}_{2_j})\int_{t-\overline{\delta}_{2_j}}^{t-\underline{\delta}_{2_j}}\dot{\boldsymbol{x}}^{\mathrm{T}}(s)\boldsymbol{P}_{4_j}\dot{\boldsymbol{x}}(s)\mathrm{d}s\\
\le&[*]\boldsymbol{\mathcal{M}}_2^j\begin{bmatrix}\boldsymbol{x}(t-\underline{\delta}_{2_j})\\ \boldsymbol{x}(t-\delta_{2_j}(t))\\ \boldsymbol{x}(t-\overline{\delta}_{2_j})\end{bmatrix},
\end{aligned}$$

where $\boldsymbol{\mathcal{M}}_1^i=\boldsymbol{M}_1^i+\mathrm{diag}\{\boldsymbol{P}_{1i},\boldsymbol{0},\boldsymbol{0}\}$ and $\boldsymbol{\mathcal{M}}_2^j=\boldsymbol{M}_2^j+\mathrm{diag}\{\boldsymbol{P}_{3j},\boldsymbol{0},\boldsymbol{0}\}$.

From Assumption 3, there exist positive diagonal matrices $\boldsymbol{T}_1$ and $\boldsymbol{T}_2$ making the following inequalities hold

$$[*]\begin{bmatrix}-2\mathscr{K}_{\mathrm{m}}\boldsymbol{T}_1\mathscr{K}_{\mathrm{M}} & \boldsymbol{T}_1(\mathscr{K}_{\mathrm{m}}+\mathscr{K}_{\mathrm{M}})\\ * & -2\boldsymbol{T}_1\end{bmatrix}\begin{bmatrix}\boldsymbol{x}_{\mathrm{e}}(t)\\ f(\boldsymbol{x}_{\mathrm{e}}(t))\end{bmatrix}\ge 0,$$

$$[*]\begin{bmatrix}-2\mathscr{K}_{\mathrm{m}}\boldsymbol{T}_2\mathscr{K}_{\mathrm{M}} & \boldsymbol{T}_2(\mathscr{K}_{\mathrm{m}}+\mathscr{K}_{\mathrm{M}})\\ * & -2\boldsymbol{T}_2\end{bmatrix}\begin{bmatrix}\boldsymbol{x}_{\mathrm{e}}(t-h(t))\\ f(\boldsymbol{x}_{\mathrm{e}}(t-h(t)))\end{bmatrix}\ge 0,$$

where $f()$ is the activation function.

Define an augmented state vector as

$$\begin{aligned}
\boldsymbol{\xi}(t)=&\mathrm{col}\{\boldsymbol{x}(t),\boldsymbol{\mathcal{X}}_1(t),\boldsymbol{\mathcal{X}}_2(t),\boldsymbol{\mathcal{X}}_3(t),\boldsymbol{\mathscr{E}}_1(t),\boldsymbol{\mathscr{E}}_2(t),\\
&\boldsymbol{\varphi}(\boldsymbol{x}(t)),\boldsymbol{\varphi}(\boldsymbol{x}(t-h(t))),\sqrt{\eta_1(t)},\\
&\sqrt{\eta_2(t)},\mathscr{G}_{\mathrm{s}}(\boldsymbol{y}(t)),\mathscr{G}_{\mathrm{c}}(\bar{\boldsymbol{u}}(t))\},
\end{aligned}\tag{22}$$

where

$$\begin{aligned}
\boldsymbol{\mathcal{X}}_1(t)=&[\boldsymbol{x}(t-\underline{\delta}_{10})\ \boldsymbol{x}(t-\delta_{10}(t))\ \boldsymbol{x}(t-\overline{\delta}_{10})\ \cdots\\
&\boldsymbol{x}(t-\underline{\delta}_{1N_1})\ \boldsymbol{x}(t-\delta_{1N_1}(t))\ \boldsymbol{x}(t-\overline{\delta}_{1N_1})],\\
\boldsymbol{\mathcal{X}}_2(t)=&[\boldsymbol{x}(t-\underline{\delta}_{20})\ \boldsymbol{x}(t-\delta_{20}(t))\ \boldsymbol{x}(t-\overline{\delta}_{20})\ \cdots\\
&\boldsymbol{x}(t-\underline{\delta}_{2N_2})\ \boldsymbol{x}(t-\delta_{2N_2}(t))\ \boldsymbol{x}(t-\overline{\delta}_{2N_2})],\\
\boldsymbol{\mathcal{X}}_3(t)=&[\boldsymbol{x}(t-h(t))\ \boldsymbol{x}(t-h_{\mathrm{M}})],\\
\boldsymbol{\mathscr{E}}_1(t)=&[\boldsymbol{e}_{10}(t)\ \boldsymbol{e}_{11}(t)\ \cdots\ \boldsymbol{e}_{1N_1}(t)],\\
\boldsymbol{\mathscr{E}}_2(t)=&[\boldsymbol{e}_{20}(t)\ \boldsymbol{e}_{21}(t)\ \cdots\ \boldsymbol{e}_{2N_2}(t)].
\end{aligned}$$

Then, from Eqs. (21) and (22), we have $\dot{V}(t)\le 0$ if and only if the subsequent inequalities are satisfied:

$$\begin{aligned}
&\sum_{l=1}^{L-1}\sum_{m\ne l}^{L}\alpha_m h_l h_m\{\boldsymbol{\Pi}_{lm}^{11}-(\boldsymbol{\Pi}_{lm}^{12})^{\mathrm{T}}\boldsymbol{\Pi}_{13}^{-1}\boldsymbol{\Pi}_{lm}^{12}\\
&+\frac{\alpha_l}{\alpha_m}[\boldsymbol{\Pi}_{ml}^{11}-(\boldsymbol{\Pi}_{ml}^{12})^{\mathrm{T}}\boldsymbol{\Pi}_{13}^{-1}\boldsymbol{\Pi}_{ml}^{12}]\}\\
&+\sum_{l=1}^{L}\alpha_l h_l^2[\boldsymbol{\Pi}_{ll}^{11}-(\boldsymbol{\Pi}_{ll}^{12})^{\mathrm{T}}\boldsymbol{\Pi}_{13}^{-1}\boldsymbol{\Pi}_{ll}^{12}]<0.
\end{aligned}$$

Using the Schur complement in Eqs. (16)–(18), SDDETM in Eqs. (4) and (5), and DOFC in Eq. (12) implies that

$$\begin{aligned}
&\boldsymbol{\Pi}_{ll}^{11}-(\boldsymbol{\Pi}_{ll}^{12})^{\mathrm{T}}\boldsymbol{\Pi}_{13}^{-1}\boldsymbol{\Pi}_{ll}^{12}<0,\\
&\boldsymbol{\Pi}_{lm}^{11}-(\boldsymbol{\Pi}_{lm}^{12})^{\mathrm{T}}\boldsymbol{\Pi}_{13}^{-1}\boldsymbol{\Pi}_{lm}^{12}+\zeta_1\boldsymbol{\Pi}_{ml}^{11}\\
&-\zeta_2(\boldsymbol{\Pi}_{ml}^{12})^{\mathrm{T}}\boldsymbol{\Pi}_{13}^{-1}\boldsymbol{\Pi}_{ml}^{12}<0,\\
&\boldsymbol{\Pi}_{lm}^{11}-(\boldsymbol{\Pi}_{lm}^{12})^{\mathrm{T}}\boldsymbol{\Pi}_{13}^{-1}\boldsymbol{\Pi}_{lm}^{12}+\zeta_2\boldsymbol{\Pi}_{ml}^{11}\\
&-\zeta_2(\boldsymbol{\Pi}_{ml}^{12})^{\mathrm{T}}\boldsymbol{\Pi}_{13}^{-1}\boldsymbol{\Pi}_{ml}^{12}<0.
\end{aligned}$$

Considering $(\zeta_2-\frac{\alpha_l}{\alpha_m})(\boldsymbol{\Pi}_{ml}^{12})^{\mathrm{T}}\boldsymbol{\Pi}_{13}^{-1}\boldsymbol{\Pi}_{ml}^{12}<0$, we can obtain

$$\begin{cases}
\boldsymbol{\Pi}_{lm}^{11}-(\boldsymbol{\Pi}_{lm}^{12})^{\mathrm{T}}\boldsymbol{\Pi}_{13}^{-1}\boldsymbol{\Pi}_{lm}^{12}+\zeta_1\boldsymbol{\Pi}_{ml}^{11}\\
-\dfrac{\alpha_l}{\alpha_m}(\boldsymbol{\Pi}_{ml}^{12})^{\mathrm{T}}\boldsymbol{\Pi}_{13}^{-1}\boldsymbol{\Pi}_{ml}^{12}<0,\\
\boldsymbol{\Pi}_{lm}^{11}-(\boldsymbol{\Pi}_{lm}^{12})^{\mathrm{T}}\boldsymbol{\Pi}_{13}^{-1}\boldsymbol{\Pi}_{lm}^{12}+\zeta_2\boldsymbol{\Pi}_{ml}^{11}\\
-\dfrac{\alpha_l}{\alpha_m}(\boldsymbol{\Pi}_{ml}^{12})^{\mathrm{T}}\boldsymbol{\Pi}_{13}^{-1}\boldsymbol{\Pi}_{ml}^{12}<0.
\end{cases}\tag{23}$$

From Eqs. (14) and (23), we have $\boldsymbol{\Pi}_{lm}^{11}-(\boldsymbol{\Pi}_{lm}^{12})^{\mathrm{T}}\boldsymbol{\Pi}_{13}^{-1}\boldsymbol{\Pi}_{lm}^{12}+\frac{\alpha_l}{\alpha_m}[\boldsymbol{\Pi}_{ml}^{11}-(\boldsymbol{\Pi}_{ml}^{12})^{\mathrm{T}}\boldsymbol{\Pi}_{13}^{-1}\boldsymbol{\Pi}_{ml}^{12}]<0$. The asymptotic stability of the closed-loop system (15) can be ensured by Eqs. (16)–(18). Consequently, the proof is thereby established.

Remark 3 By referring to the research progress on delay systems in recent papers (Zhang XM et al., 2018; Chen et al., 2022), the Lyapunov functional

candidate in this study can be further improved from the following two aspects: First, the incorporation of a quadratic matrix that is affinely dependent on the delay offers a more generalized framework than the conventional constant matrix; Second, the utilization of the two double-integral terms in $V_4(t)$ to represent the interval $[t-h_{\mathrm{M}},t]$ as $[t-h_{\mathrm{M}},t-h(t)]$ and $[t-h(t),t]$, which introduces two different matrices $\boldsymbol{G}_{51}$ and $\boldsymbol{G}_{52}$. This augmented Lyapunov functional scheme has the potential to further reduce the conservatism of the design results, which will be explored in future research.

In Theorem 1, it is observed that the DOFC parameters $\boldsymbol{A}_{km}$, $\boldsymbol{B}_{km}$, $\boldsymbol{C}_{km}$, $\boldsymbol{D}_{km}$, and $\boldsymbol{F}_{km}$ are intertwined with the Lyapunov matrix $\boldsymbol{P}$, rendering the problem nonconvex and the DOFC unresolvable. Specifically, the resolution is divided into two parts: First, we decouple the DOFC parameters and matrix $\boldsymbol{P}$ in Proposition 1; Furthermore, the nonconvex LMIs are transformed into convex formulations, referring to cone complement linearization (CCL) approach in Theorem 2.

Proposition 1 For $i\in\mathcal{N}_{N_1}$, $j\in\mathcal{N}_{N_2}$, $\mathscr{B}\in\{1,2\}$, $\mathscr{C}\in\{3,4\}$, given positive scalars $\underline{\delta}_{1_i}$, $\overline{\delta}_{1_i}$, $\underline{\delta}_{2_j}$, $\overline{\delta}_{2_j}$, ϵ_{1_i}, ϵ_{2_j}, $N_{\mathscr{B}}$, $w_{\mathscr{B}}$, $\mu_{\mathscr{B}}$, $\zeta_{\mathscr{B}}$, the diagonal matrices $\mathscr{K}_{\mathrm{m}}$, $\mathscr{K}_{\mathrm{M}}$, and real matrices $\boldsymbol{G}_{\mathrm{s}}$, $\boldsymbol{G}_{\mathrm{c}}$, the closed-loop system (15) is asymptotically stable with the proposed SDDETM, if there exist positive diagonal matrices $\boldsymbol{T}_1$ and $\boldsymbol{T}_2$, and $\boldsymbol{X}$, $\boldsymbol{Y}\in\mathcal{S}_a^+$, $\tilde{\boldsymbol{P}}_{\mathscr{B}_i}$, $\tilde{\boldsymbol{P}}_{\mathscr{C}_j}$, $\tilde{\boldsymbol{P}}_5\in\mathcal{S}_n^+$, $\boldsymbol{\Phi}_{1_i}\in\mathcal{S}_c^+$, $\tilde{\boldsymbol{\Phi}}_{2_j}\in\mathcal{S}_b^+$, matrices $\tilde{\boldsymbol{X}}_{1_i}$, $\tilde{\boldsymbol{X}}_{2_j}$ and $\tilde{\boldsymbol{X}}_3$ of appropriate dimensions such that

$$\boldsymbol{\Theta}_l^{21}=\begin{bmatrix}\boldsymbol{\Pi}_{ll}^{21} & *\\ \boldsymbol{\Pi}_{ll}^{22} & \boldsymbol{\Pi}^{23}\end{bmatrix}\le 0, \tag{24}$$

$$\boldsymbol{\Theta}_{lm}^{22}=\begin{bmatrix}\boldsymbol{\Pi}_{lm}^{21}+\zeta_1\boldsymbol{\Pi}_{ml}^{21} & * & *\\ \boldsymbol{\Pi}_{lm}^{22} & \boldsymbol{\Pi}^{23} & *\\ \zeta_2\boldsymbol{\Pi}_{ml}^{22} & \boldsymbol{0} & \zeta_2\boldsymbol{\Pi}^{23}\end{bmatrix}\le 0, \tag{25}$$

$$\boldsymbol{\Theta}_{lm}^{23}=\begin{bmatrix}\boldsymbol{\Pi}_{lm}^{21}+\zeta_2\boldsymbol{\Pi}_{ml}^{21} & * & *\\ \boldsymbol{\Pi}_{lm}^{22} & \boldsymbol{\Pi}^{23} & *\\ \zeta_2\boldsymbol{\Pi}_{ml}^{22} & \boldsymbol{0} & \zeta_2\boldsymbol{\Pi}^{23}\end{bmatrix}\le 0, \tag{26}$$

$$\begin{cases}\boldsymbol{Z}=\begin{bmatrix}\boldsymbol{X} & \boldsymbol{I}\\ * & \boldsymbol{Y}\end{bmatrix}\ge 0,\ \begin{bmatrix}\tilde{\boldsymbol{P}}_{2_i} & \tilde{\boldsymbol{X}}_{1_i}\\ * & \tilde{\boldsymbol{P}}_{2_i}\end{bmatrix}\ge 0,\\ \begin{bmatrix}\tilde{\boldsymbol{P}}_{4_j} & \tilde{\boldsymbol{X}}_{2_j}\\ * & \tilde{\boldsymbol{P}}_{4_j}\end{bmatrix}\ge 0,\ \begin{bmatrix}\tilde{\boldsymbol{P}}_5 & \tilde{\boldsymbol{X}}_3\\ * & \tilde{\boldsymbol{P}}_5\end{bmatrix}\ge 0,\end{cases} \tag{27}$$

where

$$\boldsymbol{\Pi}_{lm}^{21}=\begin{bmatrix}\boldsymbol{\gamma}_{lm}^{11} & \boldsymbol{\gamma}_{lm}^{12} & \boldsymbol{\gamma}_{lm}^{13} & \boldsymbol{\gamma}_l^{14} & \boldsymbol{0} & \boldsymbol{\psi}_l^7 & \boldsymbol{\psi}_l^8\\ * & \boldsymbol{\gamma}_l^{22} & \boldsymbol{0} & \boldsymbol{\gamma}_l^{24} & \boldsymbol{0} & \boldsymbol{0} & \boldsymbol{0}\\ * & * & \boldsymbol{\beta}^{33} & \boldsymbol{0} & \boldsymbol{0} & \boldsymbol{0} & \boldsymbol{0}\\ * & * & * & \boldsymbol{\beta}^{44} & \boldsymbol{0} & \boldsymbol{0} & \boldsymbol{0}\\ * & * & * & * & \boldsymbol{\beta}^{55} & \boldsymbol{0} & \boldsymbol{0}\\ * & * & * & * & * & -w_1\boldsymbol{I} & \boldsymbol{0}\\ * & * & * & * & * & * & -w_2\boldsymbol{I}\end{bmatrix},$$

$$\begin{aligned}\boldsymbol{\gamma}_{lm}^{11}&=\mathrm{He}(\boldsymbol{\psi}_{lm}^0)-\sum_{i=0}^{N_1}\tilde{\boldsymbol{P}}_{1i}-\sum_{j=0}^{N_2}\tilde{\boldsymbol{P}}_{3j}-\tilde{\boldsymbol{P}}_5\\&\quad-2\boldsymbol{J}_1^{\mathrm{T}}\boldsymbol{E}_1^{\mathrm{T}}\mathscr{K}_{\mathrm{m}}^{\mathrm{T}}\boldsymbol{T}_1\mathscr{K}_{\mathrm{M}}\boldsymbol{J}_1\boldsymbol{E}_1,\\ \boldsymbol{\gamma}_{lm}^{12}&=[\boldsymbol{P}\tilde{\boldsymbol{\mathcal{A}}}_{lm}^1+[\tilde{\boldsymbol{\vartheta}}_{lm}^{10}\ \cdots\ \tilde{\boldsymbol{\vartheta}}_{lm}^{1N_1}],\ \boldsymbol{P}\tilde{\boldsymbol{\mathcal{A}}}_{lm}^2+\\&\quad[\tilde{\boldsymbol{\vartheta}}_{lm}^{20}\ \cdots\ \tilde{\boldsymbol{\vartheta}}_{lm}^{2N_2}],\tilde{\boldsymbol{P}}_5-\tilde{\boldsymbol{X}}_3^{\mathrm{T}},\ \tilde{\boldsymbol{X}}_3^{\mathrm{T}}],\\ \boldsymbol{\vartheta}_{lm}^{1i}&=[\tilde{\boldsymbol{P}}_{1i}\ \boldsymbol{0}_{n,2n}],\ \boldsymbol{\vartheta}_{lm}^{2j}=[\tilde{\boldsymbol{P}}_{3j}\ \boldsymbol{0}_{n,2n}],\\ \tilde{\boldsymbol{\mathcal{A}}}_{lm}^1&=[\boldsymbol{0}_n\ \boldsymbol{\psi}_{lm}^1\ \boldsymbol{0}_{n,(3N_1+1)n}],\\ \tilde{\boldsymbol{\mathcal{A}}}_{lm}^2&=[\boldsymbol{0}_n\ \boldsymbol{\psi}_{lm}^2\ \boldsymbol{0}_{n,(3N_2+1)n}],\\ \boldsymbol{\gamma}_{lm}^{13}&=[\boldsymbol{\psi}_m^3\ \boldsymbol{0}_{n,N_1c}\ \boldsymbol{\psi}_l^4\ \boldsymbol{0}_{n,N_2b}],\\ \boldsymbol{\gamma}_l^{14}&=[\boldsymbol{\psi}_l^5+\boldsymbol{J}_1^{\mathrm{T}}\boldsymbol{E}_1^{\mathrm{T}}\boldsymbol{T}_1(\mathscr{K}_{\mathrm{m}}+\mathscr{K}_{\mathrm{M}})\ \boldsymbol{\psi}_l^6],\\ \boldsymbol{\gamma}_l^{22}&=\mathrm{diag}\{\tilde{\boldsymbol{M}}_{10},\tilde{\boldsymbol{M}}_{11},\cdots,\tilde{\boldsymbol{M}}_{1N_1},\\&\quad\tilde{\boldsymbol{M}}_{20},\tilde{\boldsymbol{M}}_{21},\cdots,\tilde{\boldsymbol{M}}_{2N_2},\tilde{\boldsymbol{M}}_3\},\end{aligned}$$

$$\tilde{\boldsymbol{M}}_{1i}=\begin{bmatrix}-\tilde{\boldsymbol{P}}_{1i}-\tilde{\boldsymbol{P}}_{2i} & \tilde{\boldsymbol{P}}_{2i}-\tilde{\boldsymbol{X}}_{1i}^{\mathrm{T}} & \tilde{\boldsymbol{X}}_{1i}^{\mathrm{T}}\\ * & -2\tilde{\boldsymbol{P}}_{2i}+\mathrm{He}(\tilde{\boldsymbol{X}}_{1i}) & \tilde{\boldsymbol{P}}_{2i}-\tilde{\boldsymbol{X}}_{1i}^{\mathrm{T}}\\ * & * & -\tilde{\boldsymbol{P}}_{2i}\end{bmatrix},$$

$$\tilde{\boldsymbol{M}}_{2j}=\begin{bmatrix}-\tilde{\boldsymbol{P}}_{3j}-\tilde{\boldsymbol{P}}_{4j} & \tilde{\boldsymbol{P}}_{4j}-\tilde{\boldsymbol{X}}_{2j}^{\mathrm{T}} & \tilde{\boldsymbol{X}}_{2j}^{\mathrm{T}}\\ * & -2\tilde{\boldsymbol{P}}_{4j}+\mathrm{He}(\tilde{\boldsymbol{X}}_{2j}) & \tilde{\boldsymbol{P}}_{4j}-\tilde{\boldsymbol{X}}_{2j}^{\mathrm{T}}\\ * & * & -\tilde{\boldsymbol{P}}_{4j}\end{bmatrix},$$

$$\tilde{\boldsymbol{M}}_3=\begin{bmatrix}-2\tilde{\boldsymbol{P}}_5+\mathrm{He}(\tilde{\boldsymbol{X}}_3) & & \\ -2\boldsymbol{J}_1^{\mathrm{T}}\boldsymbol{E}_1^{\mathrm{T}}\mathscr{K}_{\mathrm{m}}^{\mathrm{T}}\boldsymbol{T}_2\mathscr{K}_{\mathrm{M}}\boldsymbol{E}_1\boldsymbol{J}_1 & \tilde{\boldsymbol{P}}_5-\tilde{\boldsymbol{X}}_3^{\mathrm{T}} & \\ * & & -\tilde{\boldsymbol{P}}_5\end{bmatrix},$$

$$\boldsymbol{\gamma}_l^{24}=\begin{bmatrix}\boldsymbol{0}_{3(N_1+N_2+2)n,a} & \boldsymbol{0}_{3(N_1+N_2+2)n,a}\\ \boldsymbol{0}_{2n,a} & [(\mathscr{K}_{\mathrm{m}}+\mathscr{K}_{\mathrm{M}})^{\mathrm{T}}\boldsymbol{T}_2^{\mathrm{T}}\boldsymbol{E}_1^{\mathrm{T}}\boldsymbol{J}_1^{\mathrm{T}}\ \boldsymbol{0}_{a,n}]^{\mathrm{T}}\end{bmatrix},$$

$$\begin{aligned}\boldsymbol{\Pi}_{lm}^{22}&=[(\tilde{\boldsymbol{F}}_{lm}^1)^{\mathrm{T}}\boldsymbol{\mathcal{D}}\ \ (\tilde{\boldsymbol{F}}_{lm}^2)^{\mathrm{T}}\ \ (\tilde{\boldsymbol{F}}_l^3)^{\mathrm{T}}\ \ (\tilde{\boldsymbol{F}}_m^4)^{\mathrm{T}}]^{\mathrm{T}},\\ \tilde{\boldsymbol{F}}_{lm}^1&=[\boldsymbol{\psi}_{lm}^0\ \tilde{\mathcal{A}}_{lm}^1\ \tilde{\mathcal{A}}_{lm}^2\ \boldsymbol{0}_{n,2n}\ \boldsymbol{\gamma}_l^{13}\ \boldsymbol{\psi}_l^5\\&\quad\boldsymbol{\psi}_l^6\ \boldsymbol{0}_{n,2}\ \boldsymbol{\psi}_l^7\ \boldsymbol{\psi}_l^8],\\ \tilde{\boldsymbol{F}}_{lm}^2&=\mathrm{col}\{\tilde{\boldsymbol{H}}_{10},\ \tilde{\boldsymbol{H}}_{11},\ \cdots,\ \tilde{\boldsymbol{H}}_{1N_1},\\&\quad\tilde{\boldsymbol{H}}_{20},\ \tilde{\boldsymbol{H}}_{21},\ \cdots,\ \tilde{\boldsymbol{H}}_{2N_2}\},\\ \tilde{\boldsymbol{H}}_{1i}&=[\boldsymbol{0}_{c,(3i-1)n}\ \boldsymbol{\psi}_l^9\ \boldsymbol{0}_{c,[3(N_1+N_2-i)+10]n+N}],\\&\quad i\in\mathcal{N}_{N_1},\end{aligned}$$

$$\tilde{\boldsymbol{H}}_{2j}=[\boldsymbol{0}_{b,[3(N_1+j)+2]n}\ \boldsymbol{\psi}_m^{10}\ \boldsymbol{0}_{b,[3(N_2-j)+7]n+N}],\quad j\in\mathcal{N}_{N_2},$$
$$(\tilde{\boldsymbol{F}}_l^3)^{\mathrm{T}}=[\boldsymbol{0}_{c,2n}\ \boldsymbol{G}_{\mathrm{s}}\boldsymbol{\psi}_l^9\ \boldsymbol{0}_{c,[3(N_1+N_2)+6]n}\ \boldsymbol{G}_{\mathrm{s}}\ \boldsymbol{0}_{c,N+n-c}],$$
$$(\tilde{\boldsymbol{F}}_m^4)^{\mathrm{T}}=[\boldsymbol{0}_{b,(3N_1+5)n}\ \boldsymbol{G}_{\mathrm{c}}\boldsymbol{\psi}_m^{10}\ \boldsymbol{0}_{b,(3N_2+3)n+(N_1+1)c}\ \boldsymbol{G}_{\mathrm{c}}\ \boldsymbol{0}_{b,(N_2+1)b+n+c+2}],$$
$$\boldsymbol{\Pi}^{23}=\mathrm{diag}\{\tilde{\boldsymbol{\mathcal{E}}},(\boldsymbol{\Delta}\boldsymbol{\beta}^{33})^{-1},-\boldsymbol{I},-\boldsymbol{I}\},$$
$$\tilde{\boldsymbol{\mathcal{E}}}=-\mathrm{diag}\{\boldsymbol{Z}\tilde{\boldsymbol{P}}_{10}^{-1}\boldsymbol{Z},\cdots,\boldsymbol{Z}\tilde{\boldsymbol{P}}_{1N_1}^{-1}\boldsymbol{Z},\boldsymbol{Z}\tilde{\boldsymbol{P}}_{20}^{-1}\boldsymbol{Z},\cdots,\boldsymbol{Z}\tilde{\boldsymbol{P}}_{2N_1}^{-1}\boldsymbol{Z},\boldsymbol{Z}\tilde{\boldsymbol{P}}_{30}^{-1}\boldsymbol{Z},\cdots,\boldsymbol{Z}\tilde{\boldsymbol{P}}_{3N_2}^{-1}\boldsymbol{Z},\boldsymbol{Z}\tilde{\boldsymbol{P}}_{40}^{-1}\boldsymbol{Z},\cdots,\boldsymbol{Z}\tilde{\boldsymbol{P}}_{4N_2}^{-1}\boldsymbol{Z},\boldsymbol{Z}\tilde{\boldsymbol{P}}_{5}^{-1}\boldsymbol{Z}\},$$

with

$$\boldsymbol{J}_1=\begin{bmatrix}\boldsymbol{X}&\boldsymbol{I}\\ \boldsymbol{X}&\boldsymbol{0}\end{bmatrix},\ \boldsymbol{J}_2=\begin{bmatrix}\boldsymbol{I}&\boldsymbol{Y}\\ \boldsymbol{0}&\boldsymbol{N}^{\mathrm{T}}\end{bmatrix},$$
$$\boldsymbol{\psi}_{lm}^0=\begin{bmatrix}\boldsymbol{A}_l\boldsymbol{X}&\boldsymbol{A}_l\\ \boldsymbol{\varpi}_{lm}^1&\boldsymbol{Y}\boldsymbol{A}_l\end{bmatrix},\ \boldsymbol{\psi}_{lm}^1=\begin{bmatrix}\boldsymbol{0}&\boldsymbol{0}\\ \boldsymbol{\varpi}_{lm}^3&b^s\boldsymbol{\varpi}_m^2\boldsymbol{D}_l\end{bmatrix},$$
$$\boldsymbol{\psi}_{lm}^2=\begin{bmatrix}\boldsymbol{E}_l\boldsymbol{\varpi}_m^4&\boldsymbol{0}\\ \boldsymbol{\varpi}_{lm}^5&\boldsymbol{0}\end{bmatrix},\boldsymbol{\psi}_m^3=\begin{bmatrix}\boldsymbol{0}\\ b^s\boldsymbol{\varpi}_m^2\end{bmatrix},$$
$$\boldsymbol{\psi}_l^4=\begin{bmatrix}b^c\boldsymbol{E}_l\\ b^c\boldsymbol{Y}\boldsymbol{E}_l\end{bmatrix},\boldsymbol{\psi}_l^5=\begin{bmatrix}\boldsymbol{B}_l&\boldsymbol{0}\\ \boldsymbol{Y}\boldsymbol{B}_l&\boldsymbol{0}\end{bmatrix},$$
$$\boldsymbol{\psi}_l^6=\begin{bmatrix}\boldsymbol{C}_l&\boldsymbol{0}\\ \boldsymbol{Y}\boldsymbol{C}_l&\boldsymbol{0}\end{bmatrix},\ \boldsymbol{\psi}_m^7=\begin{bmatrix}\boldsymbol{0}\\ (1-b^s)\boldsymbol{\varpi}_m^2\end{bmatrix},$$
$$\boldsymbol{\psi}_l^8=\begin{bmatrix}(1-b^s)\boldsymbol{E}_l\\ (1-b^s)\boldsymbol{Y}\boldsymbol{E}_l\end{bmatrix},\ \boldsymbol{\psi}_l^9=\begin{bmatrix}\boldsymbol{D}_l\boldsymbol{X}&\boldsymbol{D}_l\end{bmatrix},$$
$$\boldsymbol{\psi}_m^{10}=\begin{bmatrix}\boldsymbol{\varpi}_m^4&\boldsymbol{0}\end{bmatrix}.$$

Proof Partition the Lyapunov matrix $\boldsymbol{P}=\begin{bmatrix}\boldsymbol{Y}&\boldsymbol{N}\\ \boldsymbol{N}^{\mathrm{T}}&\boldsymbol{Y}_1\end{bmatrix}$, where $\boldsymbol{N}=\boldsymbol{X}^{-1}-\boldsymbol{Y}$ and $\boldsymbol{Y}_1=\boldsymbol{N}^{\mathrm{T}}(\boldsymbol{Y}-\boldsymbol{X}^{-1})^{-1}\boldsymbol{N}$. Without loss of generality, we assume that $\boldsymbol{N}$ is nonsingular (Zhang XM and Han, 2014). Obviously, since $\boldsymbol{Y}_1>0$ and $\boldsymbol{Y}-\boldsymbol{X}^{-1}>0$, thus $\boldsymbol{Z}>0$ by Schur complement. It is noted that considering the definitions of $\boldsymbol{J}_1$, $\boldsymbol{J}_2$, and $\boldsymbol{N}$, the equation $\boldsymbol{J}_2=\boldsymbol{P}\boldsymbol{J}_1$ holds. Moreover, we define

$$\boldsymbol{\mathcal{J}}_1\triangleq\mathrm{diag}\{\overbrace{\boldsymbol{J}_1,\cdots,\boldsymbol{J}_1}^{3(N_1+N_2)+9},\overbrace{\boldsymbol{I}_c,\cdots,\boldsymbol{I}_c}^{N_1+1},\overbrace{\boldsymbol{I}_b,\cdots,\boldsymbol{I}_b}^{N_2+1},\boldsymbol{I}_n,\boldsymbol{I}_n,\boldsymbol{I},\boldsymbol{I},\boldsymbol{I}_c,\boldsymbol{I}_b,\overbrace{\boldsymbol{J}_2,\cdots,\boldsymbol{J}_2}^{2(N_1+N_2)+5},\overbrace{\boldsymbol{I}_c,\cdots,\boldsymbol{I}_c}^{N_1+1},\overbrace{\boldsymbol{I}_b,\cdots,\boldsymbol{I}_b}^{N_2+1},\boldsymbol{I}_c,\boldsymbol{I}_b\},$$
$$\boldsymbol{\mathcal{J}}_2\triangleq\mathrm{diag}\{\boldsymbol{\mathcal{J}}_1,\overbrace{\boldsymbol{J}_2,\cdots,\boldsymbol{J}_2}^{2(N_1+N_2)+5},\overbrace{\boldsymbol{I}_c,\cdots,\boldsymbol{I}_c}^{N_1+1},\overbrace{\boldsymbol{I}_b,\cdots,\boldsymbol{I}_b}^{N_2+1},\boldsymbol{I}_c,\boldsymbol{I}_b\},$$

$\boldsymbol{\varpi}_{lm}^1\triangleq(\boldsymbol{Y}\boldsymbol{A}_l-\boldsymbol{N}\boldsymbol{A}_{km})\boldsymbol{X}$, $\boldsymbol{\varpi}_m^2\triangleq\boldsymbol{N}\boldsymbol{D}_{km}$, $\boldsymbol{\varpi}_{lm}^3\triangleq(b^s\boldsymbol{\varpi}_m^2\boldsymbol{D}_l+\boldsymbol{N}\boldsymbol{B}_{km})\boldsymbol{X}$, $\boldsymbol{\varpi}_m^4\triangleq\boldsymbol{F}_{km}\boldsymbol{X}$, and $\boldsymbol{\varpi}_{lm}^5\triangleq\boldsymbol{Y}\boldsymbol{E}_l\boldsymbol{\varpi}_m^4+\boldsymbol{N}\boldsymbol{C}_{km}\boldsymbol{X}$.

Perform congruence transformation on $\boldsymbol{\Theta}_l^2$ using the matrix $\boldsymbol{\mathcal{J}}$, such that $\tilde{\boldsymbol{P}}_{\mathscr{B}_1}=\boldsymbol{J}_1^{\mathrm{T}}\boldsymbol{P}_{\mathscr{B}_i}\boldsymbol{J}_1$, $\tilde{\boldsymbol{P}}_{\mathscr{C}_j}=\boldsymbol{J}_1^{\mathrm{T}}\boldsymbol{P}_{\mathscr{C}_j}\boldsymbol{J}_1$, $\tilde{\boldsymbol{P}}_5=\boldsymbol{J}_1^{\mathrm{T}}\boldsymbol{P}_5\boldsymbol{J}_1$, $\tilde{\boldsymbol{X}}_{1_i}=\boldsymbol{J}_1^{\mathrm{T}}\boldsymbol{X}_{1_i}\boldsymbol{J}_1$, $\tilde{\boldsymbol{X}}_{2_j}=\boldsymbol{J}_1^{\mathrm{T}}\boldsymbol{X}_{2_j}\boldsymbol{J}_1$, and $\tilde{\boldsymbol{X}}_3=\boldsymbol{J}_1^{\mathrm{T}}\boldsymbol{X}_{2_j}\boldsymbol{J}_1$. Subsequently, after some simple algebraic manipulations, we have

$$\boldsymbol{\mathcal{J}}_1^{\mathrm{T}}\boldsymbol{\Theta}_l^{11}\boldsymbol{\mathcal{J}}_1=\boldsymbol{\Theta}_l^{21},$$
$$\boldsymbol{\mathcal{J}}_2^{\mathrm{T}}\boldsymbol{\Theta}_{lm}^{12}\boldsymbol{\mathcal{J}}_2=\boldsymbol{\Theta}_{lm}^{22},$$
$$\boldsymbol{\mathcal{J}}_2^{\mathrm{T}}\boldsymbol{\Theta}_{lm}^{13}\boldsymbol{\mathcal{J}}_2=\boldsymbol{\Theta}_{lm}^{23}.$$

Denote $\boldsymbol{P}=\boldsymbol{J}_2\boldsymbol{J}_1^{-1}$, $\boldsymbol{P}_{\mathscr{B}_i}=\boldsymbol{J}_1^{-\mathrm{T}}\tilde{\boldsymbol{P}}_{\mathscr{B}_i}\boldsymbol{J}_1^{-1}$, $\boldsymbol{P}_{\mathscr{C}_j}=\boldsymbol{J}_1^{-\mathrm{T}}\tilde{\boldsymbol{P}}_{\mathscr{C}_j}\boldsymbol{J}_1^{-1}$, $\boldsymbol{P}_5=\boldsymbol{J}_1^{-\mathrm{T}}\tilde{\boldsymbol{P}}_5\boldsymbol{J}_1^{-1}$, $\boldsymbol{X}_{1_i}=\boldsymbol{J}_1^{-\mathrm{T}}\tilde{\boldsymbol{X}}_{1_i}\boldsymbol{J}_1^{-1}$, $\boldsymbol{X}_{2_j}=\boldsymbol{J}_1^{-\mathrm{T}}\tilde{\boldsymbol{X}}_{2_j}\boldsymbol{J}_1^{-1}$, $\boldsymbol{X}_3=\boldsymbol{J}_1^{-\mathrm{T}}\tilde{\boldsymbol{X}}_3\boldsymbol{J}_1^{-1}$,

$$\boldsymbol{A}_{km}=\boldsymbol{N}^{-1}(\boldsymbol{\varpi}_{lm}^1-\boldsymbol{Y}\boldsymbol{A}_l\boldsymbol{X})\boldsymbol{X}^{-1},$$
$$\boldsymbol{D}_{km}=\boldsymbol{N}^{-1}\boldsymbol{\varpi}_m^2,$$
$$\boldsymbol{B}_{km}=\boldsymbol{N}^{-1}(\boldsymbol{\varpi}_{lm}^3-b^s\boldsymbol{\varpi}_m^2\boldsymbol{D}_l\boldsymbol{X})\boldsymbol{X}^{-1},$$
$$\boldsymbol{F}_{km}=\boldsymbol{\varpi}_m^4\boldsymbol{X}^{-1},$$
$$\boldsymbol{C}_{km}=\boldsymbol{N}^{-1}(\boldsymbol{\varpi}_{lm}^5-\boldsymbol{Y}\boldsymbol{E}_l\boldsymbol{\varpi}_m^4)\boldsymbol{X}^{-1}.$$

Then, it is evident that $\boldsymbol{P}>0$, $\boldsymbol{\mathcal{J}}_1^{-\mathrm{T}}\boldsymbol{\Theta}_l^{21}\boldsymbol{\mathcal{J}}_1^{-1}=\boldsymbol{\Theta}_l^{11}$, $\boldsymbol{\mathcal{J}}_2^{-\mathrm{T}}\boldsymbol{\Theta}_{lm}^{22}\boldsymbol{\mathcal{J}}_2^{-1}=\boldsymbol{\Theta}_{lm}^{12}$, $\boldsymbol{\mathcal{J}}_2^{-\mathrm{T}}\boldsymbol{\Theta}_{lm}^{23}\boldsymbol{\mathcal{J}}_2^{-1}=\boldsymbol{\Theta}_{lm}^{13}$; that is, the Schur complement in Eqs. (16)–(18), SDDETM in Eqs. (4) and (5), and DOFC in Eq. (12) can be ensured by Eqs. (24)–(26), which completes the proof.

Theorem 2 For $i\in\mathcal{N}_{N_1}$, $j\in\mathcal{N}_{N_2}$, $\mathscr{B}\in\{1,2\}$, $\mathscr{C}\in\{3,4\}$, given positive scalars $\underline{\delta}_{1_i}$, $\overline{\delta}_{1_i}$, $\underline{\delta}_{2_j}$, $\overline{\delta}_{2_j}$, ϵ_{1_i}, ϵ_{2_j}, $N_{\mathscr{B}}$, $w_{\mathscr{B}}$, $\mu_{\mathscr{B}}$, $\zeta_{\mathscr{B}}$, and the diagonal matrices $\mathscr{K}_{\mathrm{m}}$, $\mathscr{K}_{\mathrm{M}}$, and real matrices $\boldsymbol{G}_{\mathrm{s}}$, $\boldsymbol{G}_{\mathrm{c}}$, if there exist positive diagonal matrices $\boldsymbol{T}_1$ and $\boldsymbol{T}_2$, and $\boldsymbol{P}_{\mathscr{B}_i}$, $\bar{\boldsymbol{P}}_{\mathscr{B}_i}$, $\boldsymbol{Q}_{\mathscr{B}_i}$, $\bar{\boldsymbol{Q}}_{\mathscr{B}_i}$, $\boldsymbol{P}_{\mathscr{C}_j}$, $\bar{\boldsymbol{P}}_{\mathscr{C}_j}$, $\boldsymbol{Q}_{\mathscr{C}_j}$, $\bar{\boldsymbol{Q}}_{\mathscr{C}_j}$, $\boldsymbol{Q}_5$, $\bar{\boldsymbol{Q}}_5$, $\boldsymbol{Q}_6$, $\bar{\boldsymbol{Q}}_6$, $\boldsymbol{Q}_7$, $\bar{\boldsymbol{Q}}_7$, $\bar{\boldsymbol{Z}}\in\mathcal{S}_n^+$, $\bar{\boldsymbol{\Phi}}_{1_i}\in\mathcal{S}_c^+$, $\bar{\boldsymbol{\Phi}}_{2_j}\in\mathcal{S}_b^+$, then the stabilization problem of closed-loop system (15) integrating DOFC and SDDETM is solvable if Eq. (27) and the following inequalities are satisfied:

$$\boldsymbol{\Theta}_l^{31}=\begin{bmatrix}\boldsymbol{\Pi}_{ll}^{31}&*\\ \boldsymbol{\Pi}_{ll}^{22}&\boldsymbol{\Pi}^{33}\end{bmatrix}\le 0, \tag{28}$$

$$\boldsymbol{\Theta}_{lm}^{32}=\begin{bmatrix}\boldsymbol{\Pi}_{lm}^{31}+\zeta_1\boldsymbol{\Pi}_{ml}^{21}&*&*\\ \boldsymbol{\Pi}_{lm}^{22}&\boldsymbol{\Pi}^{33}&*\\ \zeta_2\boldsymbol{\Pi}_{ml}^{22}&\boldsymbol{0}&\zeta_2\boldsymbol{\Pi}^{33}\end{bmatrix}\le 0, \tag{29}$$

$$\boldsymbol{\Theta}_{lm}^{33}=\begin{bmatrix}\boldsymbol{\Pi}_{lm}^{31}+\zeta_2\boldsymbol{\Pi}_{ml}^{21}&*&*\\ \boldsymbol{\Pi}_{lm}^{22}&\boldsymbol{\Pi}^{33}&*\\ \zeta_2\boldsymbol{\Pi}_{ml}^{22}&\boldsymbol{0}&\zeta_2\boldsymbol{\Pi}^{33}\end{bmatrix}\le 0, \tag{30}$$

where

$$\boldsymbol{\Pi}_{lm}^{31}=\begin{bmatrix}\varsigma_{lm}^{11}&\boldsymbol{\gamma}_{lm}^{12}&\boldsymbol{\gamma}_{lm}^{13}&\boldsymbol{\gamma}_{l}^{14}&\boldsymbol{0}&\boldsymbol{\psi}_{l}^{7}&\boldsymbol{\psi}_{l}^{8}\\ *&\varsigma_{l}^{22}&\boldsymbol{0}&\boldsymbol{\gamma}_{l}^{24}&\boldsymbol{0}&\boldsymbol{0}&\boldsymbol{0}\\ *&*&\boldsymbol{\beta}^{33}&\boldsymbol{0}&\boldsymbol{0}&\boldsymbol{0}&\boldsymbol{0}\\ *&*&*&\boldsymbol{\beta}^{44}&\boldsymbol{0}&\boldsymbol{0}&\boldsymbol{0}\\ *&*&*&*&\boldsymbol{\beta}^{55}&\boldsymbol{0}&\boldsymbol{0}\\ *&*&*&*&*&-w_1\boldsymbol{I}&\boldsymbol{0}\\ *&*&*&*&*&*&-w_2\boldsymbol{I}\end{bmatrix},$$

$$\varsigma_{lm}^{11}=\mathrm{He}(\boldsymbol{\psi}_{l}^{0})-\sum_{i=0}^{N_1}\tilde{\boldsymbol{P}}_{1i}-\sum_{j=0}^{N_2}\tilde{\boldsymbol{P}}_{3j}-\tilde{\boldsymbol{P}}_{5}-2\boldsymbol{Q}_{6},$$

$$\begin{aligned}\varsigma_{l}^{22}=&\,\mathrm{diag}\{\tilde{\boldsymbol{M}}_{10},\tilde{\boldsymbol{M}}_{11},\cdots,\tilde{\boldsymbol{M}}_{1N_1},\tilde{\boldsymbol{M}}_{20},\\&\tilde{\boldsymbol{M}}_{21},\cdots,\tilde{\boldsymbol{M}}_{2N_2},\bar{\boldsymbol{M}}_{3}\},\\ \bar{\boldsymbol{M}}_{3}=&\begin{bmatrix}-2\tilde{\boldsymbol{P}}_{5}+\mathrm{He}(\tilde{\boldsymbol{X}}_{3})-2\boldsymbol{Q}_{7}&\tilde{\boldsymbol{P}}_{5}-\tilde{\boldsymbol{X}}_{3}^{\mathrm{T}}\\ *&-\tilde{\boldsymbol{P}}_{5}\end{bmatrix},\\ \boldsymbol{\Pi}^{33}=&\,\mathrm{diag}\{\bar{\boldsymbol{\mathcal{E}}},(\boldsymbol{\Delta}\bar{\boldsymbol{\beta}}^{33})^{-1},-\boldsymbol{I},-\boldsymbol{I}\},\end{aligned}$$

$$\begin{aligned}\bar{\boldsymbol{\mathcal{E}}}=&-\mathrm{diag}\{\boldsymbol{Q}_{10},\boldsymbol{Q}_{11},\cdots,\boldsymbol{Q}_{1N_1},\\&\boldsymbol{Q}_{20},\boldsymbol{Q}_{21},\cdots,\boldsymbol{Q}_{2N_1},\boldsymbol{Q}_{30},\boldsymbol{Q}_{31},\cdots,\boldsymbol{Q}_{3N_2},\\&\boldsymbol{Q}_{40},\boldsymbol{Q}_{41},\cdots,\boldsymbol{Q}_{4N_2},\boldsymbol{Q}_{5}\},\\ \bar{\boldsymbol{\beta}}^{33}=&\,\mathrm{diag}\{-\bar{\boldsymbol{\phi}}_{10},-\bar{\boldsymbol{\phi}}_{11},\cdots,-\bar{\boldsymbol{\phi}}_{1N_1},\\&-\bar{\boldsymbol{\phi}}_{20},-\bar{\boldsymbol{\phi}}_{21},\cdots,-\bar{\boldsymbol{\phi}}_{2N_2}\},\end{aligned}$$

and the following equations hold:

$$\begin{aligned}&\boldsymbol{J}_1\bar{\boldsymbol{J}}_1=\boldsymbol{I},\boldsymbol{Z}\bar{\boldsymbol{Z}}=\boldsymbol{I},\boldsymbol{Q}_{\mathscr{B}_i}\bar{\boldsymbol{Q}}_{\mathscr{B}_i}=\boldsymbol{I},\boldsymbol{Q}_{\mathscr{C}_j}\bar{\boldsymbol{Q}}_{\mathscr{C}_j}=\boldsymbol{I},\\&\tilde{\boldsymbol{P}}_{\mathscr{B}_i}\bar{\boldsymbol{P}}_{\mathscr{B}_i}=\boldsymbol{I},\tilde{\boldsymbol{P}}_{\mathscr{C}_j}\bar{\boldsymbol{P}}_{\mathscr{C}_j}=\boldsymbol{I},\tilde{\boldsymbol{P}}_{5}\bar{\boldsymbol{P}}_{5}=\boldsymbol{I},\\&\boldsymbol{\Phi}_{1_i}\bar{\boldsymbol{\Phi}}_{1_i}=\boldsymbol{I},\boldsymbol{\Phi}_{2_j}\bar{\boldsymbol{\Phi}}_{2_j}=\boldsymbol{I}.\end{aligned}\tag{31}$$

Proof Eqs. (24)–(26) contain the nonlinear terms $-\boldsymbol{Z}\tilde{\boldsymbol{P}}_{\mathscr{B}_i}^{-1}\boldsymbol{Z}$, $-\boldsymbol{Z}\tilde{\boldsymbol{P}}_{\mathscr{C}_j}^{-1}\boldsymbol{Z}$, $-\boldsymbol{Z}\tilde{\boldsymbol{P}}_{5}^{-1}\boldsymbol{Z}$, $\boldsymbol{\Phi}_{1_i}^{-1}$, and $\boldsymbol{\Phi}_{2_j}^{-1}$, and where $\mathscr{B}\in\{1,2\}$, $\mathscr{C}\in\{3,4\}$, $i\in\mathcal{N}_{N_1}$, and $j\in\mathcal{N}_{N_2}$. We use the CCL algorithm (El Ghaoui et al., 1997) to transform nonconvex linear matrix inequalities into convex optimization problems. Accordingly, the stabilization of the system (15) can be solved, leading to the DOFC. The proof is thereby established.

Remark 4 The use of the CCL algorithm in this paper significantly enhances the computational efficiency and effectiveness of the proposed method. By transforming nonconvex linear matrix inequalities into convex optimization problems, the CCL algorithm allows for the simultaneous optimization of the DOFC and SDDETM parameters. This approach not only simplifies the computational process but also yields less conservative results, ensuring robust stability and efficient resource utilization in the presence of deception attacks and time delays.

4 Simulation examples

In this section, we demonstrate two cases to evidence the effectiveness of the SDDETM. To illustrate the difference between SDDETM ($N_1>0$, $N_2>0$) and traditional ETMs ($N_1=N_2=0$), consider the following examples: In traditional ETMs, the trigger frequency is high due to the reliance on the current sample, leading to potential network congestion and Zeno behavior. In contrast, SDDETM uses past samples and internal dynamic variables, reducing trigger frequency and avoiding Zeno behavior.

4.1 Case 1

Consider NN system (15) with system matrices (Liu JL et al., 2019a):

$$\begin{aligned}&\boldsymbol{A}_1=-\begin{bmatrix}1.06&0\\0&1.06\end{bmatrix},\quad \boldsymbol{A}_2=-\begin{bmatrix}1.6&0\\0&2.3\end{bmatrix},\\&\boldsymbol{B}_1=\begin{bmatrix}0.3&-0.42\\-0.42&0.3\end{bmatrix},\quad \boldsymbol{B}_2=\begin{bmatrix}0.2&-0.32\\-0.32&0.2\end{bmatrix},\\&\boldsymbol{C}_1=\begin{bmatrix}0.3&0.3\\0.3&0.3\end{bmatrix},\quad \boldsymbol{C}_2=\begin{bmatrix}0.4&0.4\\0.4&0.4\end{bmatrix},\\&\boldsymbol{E}_1=\begin{bmatrix}-3&-0.15\\-0.75&-2\end{bmatrix},\quad \boldsymbol{E}_2=\begin{bmatrix}-0.95&-0.85\\-1.75&-0.55\end{bmatrix}.\end{aligned}$$

Suppose that the transition probabilities are

$$\begin{cases}\boldsymbol{\pi}=[\pi_{\mathscr{M}\mathscr{N}}]_{2\times2}=\begin{bmatrix}-0.3&0.3\\0.6&-0.6\end{bmatrix},\\ \boldsymbol{\rho}=[\rho_{\mathscr{P}\mathscr{Q}}]_{2\times2}=\begin{bmatrix}-0.4&-0.4\\0.65&-0.65\end{bmatrix}.\end{cases}\tag{32}$$

$f(\boldsymbol{x}_{\mathrm{e}}(t))=\mathrm{col}\{f_1(\boldsymbol{x}_{\mathrm{e}}(t)),\ f_2(\boldsymbol{x}_{\mathrm{e}}(t))\}$ is the activation function, where $f_1(\boldsymbol{x}_{\mathrm{e}}(t))=0.5\boldsymbol{x}_1(t)-\tanh(0.2\boldsymbol{x}_1(t)+0.2\boldsymbol{x}_1(t))$, $f_2(\boldsymbol{x}_{\mathrm{e}}(t))=0.95\boldsymbol{x}_2(t)-\tanh(0.75\boldsymbol{x}_1(t))$, and $\boldsymbol{\mathcal{I}}=\boldsymbol{0}$ is the input bias. $\boldsymbol{x}_{\mathrm{e}}(t)=[1.7,-2.6]^{\mathrm{T}}$ and $\boldsymbol{x}_{\mathrm{c}}(t)=[0.9,-1.9]^{\mathrm{T}}$ are the corresponding initial parameters of the system (15). The sample period h is set at 0.1 s, with the upper bound of time delays denoted as $h_{\mathrm{M}}=0.1$ s, and $\tau_{1\mathrm{M}}=\tau_{2\mathrm{M}}=0.01$ s. Using the LMI toolbox within MATLAB, we obtain

$$\boldsymbol{A}_{1k}=\begin{bmatrix}-2.911&0.150\\0.204&-2.980\end{bmatrix},\ \boldsymbol{A}_{2k}=\begin{bmatrix}-5.069&-0.096\\-0.080&-5.043\end{bmatrix},$$

$$\boldsymbol{B}_{1k}=\begin{bmatrix}-0.0715 & -0.049\\ -0.068 & -0.043\end{bmatrix},\ \boldsymbol{B}_{2k}=\begin{bmatrix}0.010 & 0.006\\ 0.008 & 0.007\end{bmatrix},$$
$$\boldsymbol{C}_{k1}=\begin{bmatrix}-0.002 & 0.003\\ 0.002 & -0.003\end{bmatrix},\ \boldsymbol{C}_{k2}=\begin{bmatrix}0.003 & -0.005\\ -0.003 & 0.004\end{bmatrix},$$
$$\boldsymbol{D}_{k1}=\begin{bmatrix}-0.021 & -0.015\\ -0.013 & -0.017\end{bmatrix},\ \boldsymbol{D}_{k2}=\begin{bmatrix}0.008 & 0.015\\ 0.018 & 0.006\end{bmatrix},$$
$$\boldsymbol{F}_{k1}=\begin{bmatrix}-0.002 & 0.003\\ 0.002 & -0.002\end{bmatrix},\ \boldsymbol{F}_{k2}=\begin{bmatrix}0.002 & -0.003\\ -0.002 & 0.003\end{bmatrix}, \tag{33}$$

and the SDDETM parameters are

$$\boldsymbol{\Phi}_{1_0}=\begin{bmatrix}25.024 & 11.991\\ 11.991 & 24.495\end{bmatrix},\boldsymbol{\Phi}_{2_0}=\begin{bmatrix}65.921 & 40.767\\ 40.767 & 65.966\end{bmatrix}. \tag{34}$$

With Eqs. (33) and (34), the state trajectories of the close system (15) with $N_1=N_2\in\{0,2,4\}$ are depicted in Fig. 2. Clearly, the state trajectories converge to zero within 10 s, demonstrating the efficacy of the designed DOFC in stabilizing the system.

When $N_1>0$ and $N_2>0$, the SDDETM incorporates previous samples, and there exist multiple triggering thresholds ϵ_{1_i} and ϵ_{2_j}, where $i\in\mathcal{N}_{N_1}$ and $j\in\mathcal{N}_{N_2}$. As these thresholds are predefined, we initiate a loop for each threshold. Specifically, we search for thresholds within the range of $[0.05,0.50]$ with the step size of 0.05. For each pair of ϵ_{1_i} and ϵ_{2_j}, the triggers generated by SDDETM 1 and SDDETM 2 are documented. Table 1 presents two cases from the comprehensive results. For different triggering thresholds in Table 1, we have the following observations: When $N_1=N_2\in\{0,2,4\}$, the SDDETM reduces the signal transmission in Network 1 by 44%, 50%, 61%, and in Network 2 by 31%, 35%, 40%, respectively. It is evident that as N_1 and N_2 rise, the communication resources can be saved. The release intervals that illustrate the results of SDDETM 1 and SDDETM 2 for $N_1=N_2\in\{0,2,4\}$ are presented in Fig. 2. Analysis of Table 1 and Fig. 2 reveals that the number of triggers released by both SDDETMs decreases as N_1 and N_2 increase. This means that with appropriately selected triggering thresholds, network resources can be preserved as N_1 and N_2 rise. Thus, the efficiency of the SDDETM is demonstrated.

4.2 Case 2

Consider two IF-THEN rules to simulate the T–S fuzzy neural network system, namely $l=2$. Let $h_1(\boldsymbol{\theta}_1(t))=\sin^2(t)$ and $h_2(\boldsymbol{\theta}_1(t))=1-h_1(\boldsymbol{\theta}_1(t))$. The parameters for the T–S neural network system (15) are as follows (Tan et al., 2020):

$$\boldsymbol{A}_1=-\begin{bmatrix}3.9 & 0\\ 0 & 3.1\end{bmatrix},\boldsymbol{A}_2=-\begin{bmatrix}4.1 & 0\\ 0 & 5.9\end{bmatrix},$$
$$\boldsymbol{B}_1=\begin{bmatrix}0.9 & -0.3\\ -0.2 & 0.5\end{bmatrix},\boldsymbol{B}_2=\begin{bmatrix}0.8 & -0.1\\ -0.3 & 0.6\end{bmatrix},$$
$$\boldsymbol{C}_1=\begin{bmatrix}0.8 & 0.2\\ 0.2 & 0.3\end{bmatrix},\ \boldsymbol{C}_2=\begin{bmatrix}0.7 & 0.1\\ 0.1 & 0.4\end{bmatrix},$$
$$\boldsymbol{E}_1=\begin{bmatrix}0.3 & 0\\ 0 & 0.8\end{bmatrix},\ \boldsymbol{E}_2=\begin{bmatrix}0.6 & 0\\ 0 & 0.5\end{bmatrix}.$$

Suppose that the neuron activation function is given as $f(\boldsymbol{x}_{\mathrm{e}}(t))=\mathrm{col}\{f_1(\boldsymbol{x}_{\mathrm{e}}(t)),\ f_2(\boldsymbol{x}_{\mathrm{e}}(t))\}$,

Table 1 Total triggers generated by SDDETM with different N_1 and N_2 values in Case 1

$N_1=N_2$	N_{trigger}			$\epsilon_{1_i}\ (i\in\mathcal{N}_{N_1})$	$\epsilon_{2_j}\ (j\in\mathcal{N}_{N_2})$
	SDDETM 1	SDDETM 2	Total		
0 (Liu JL et al., 2019a)	56	69	125	0.05	0.05
1	54	65	119	0.05, 0.10	0.05, 0.30
2	52	64	116	0.05, 0.10, 0.10	0.05, 0.30, 0.30
3	50	63	113	0.05, 0.10, 0.10, 0.20	0.05, 0.30, 0.30, 0.15
4	49	60	109	0.05, 0.10, 0.10, 0.20, 0.15	0.05, 0.30, 0.30, 0.15, 0.50
$N_1=N_2$	N_{trigger}			$\epsilon_{1_i}\ (i\in\mathcal{N}_{N_1})$	$\epsilon_{2_j}\ (j\in\mathcal{N}_{N_2})$
	SDDETM 1	SDDETM 2	Total		
0 (Liu JL et al., 2019a)	56	69	125	0.05	0.05
1	55	66	121	0.05, 0.50	0.05, 0.30
2	50	65	115	0.05, 0.50, 0.50	0.05, 0.30, 0.30
3	48	61	109	0.05, 0.50, 0.50, 0.50	0.05, 0.30, 0.30, 0.15
4	39	60	99	0.05, 0.50, 0.50, 0.50, 0.45	0.05, 0.30, 0.30, 0.15, 0.50

N_{trigger}: number of triggers

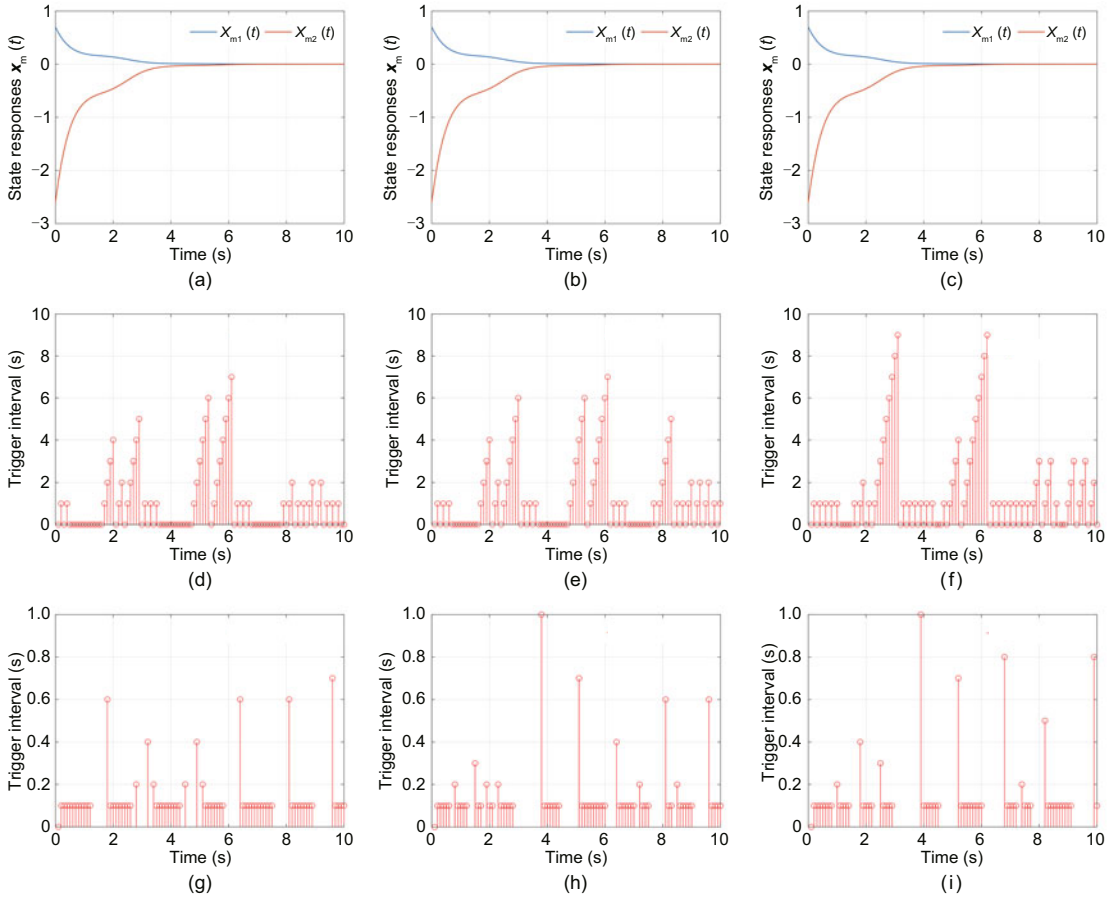

Fig. 2 The state trajectories and release time intervals of SDDETM 1 and SDDETM 2 in Case 1, for state trajectories with $N_1 = N_2 = 0$ (a), $N_1 = N_2 = 2$ (b), and $N_1 = N_2 = 4$ (c), for SDDETM 1 with $N_1 = N_2 = 0$ (d), $N_1 = N_2 = 2$ (e), $N_1 = N_2 = 4$ (f), and for SDDETM 2 with $N_1 = N_2 = 0$ (g), $N_1 = N_2 = 2$ (h), and $N_1 = N_2 = 4$ (i)

where $f_1(\boldsymbol{x}_e(t)) = f_2(\boldsymbol{x}_e(t)) = 10[\sin(0.03x) - \tanh(0.02x)]$, and the input bias is given as $\boldsymbol{J} = \boldsymbol{0}$. The transition probability is given in Eq. (32). Here, we set $h_M = 0.1$ s, $h = 0.1$ s, $\mathscr{K}_m = \boldsymbol{0}$, and $\mathscr{K}_M = \boldsymbol{I}$. The nonlinear functions of the deception attacks in sampler–DOFC and DOFC–ZOH are $\mathscr{G}_s(\boldsymbol{y}_e(t)) = -\tanh(0.2\boldsymbol{y}_e(t))$ and $\mathscr{G}_c(\bar{\boldsymbol{u}}(t)) = -\tanh(0.2\bar{\boldsymbol{u}}(t))$, respectively. According to Theorem 2 and the LMI toolbox for Eq. (27) and Eqs. (28)–(30), the DOFC parameters are obtained as follows:

$$\boldsymbol{A}_{1k} = \begin{bmatrix} -4.973 & 0.064 \\ -0.087 & -4.449 \end{bmatrix}, \boldsymbol{A}_{2k} = \begin{bmatrix} -9.287 & -0.013 \\ 0.009 & -7.444 \end{bmatrix},$$

$$\boldsymbol{B}_{1k} = \begin{bmatrix} -0.002 & 2.150 \\ 0.000 & -0.007 \end{bmatrix}, \boldsymbol{B}_{2k} = \begin{bmatrix} 0.005 & -0.003 \\ -7.001 & 0.001 \end{bmatrix},$$

$$\boldsymbol{C}_{k1} = \begin{bmatrix} 0.017 & 0.000 \\ 0.000 & -0.016 \end{bmatrix}, \boldsymbol{C}_{k2} = \begin{bmatrix} -0.036 & 0.001 \\ 2.344 & 0.033 \end{bmatrix},$$

$$\boldsymbol{D}_{k1} = \begin{bmatrix} 0.010 & 0.000 \\ 0.000 & 0.007 \end{bmatrix}, \boldsymbol{D}_{k2} = \begin{bmatrix} 0.011 & 0.000 \\ 0.000 & -0.001 \end{bmatrix},$$

$$\boldsymbol{F}_{k1} = \begin{bmatrix} 0.0124 & 0.000 \\ 0.000 & -0.013 \end{bmatrix}, \boldsymbol{F}_{k2} = \begin{bmatrix} -0.016 & 0.000 \\ 0.000 & 0.016 \end{bmatrix},$$

and the SDDETM parameters are

$$\boldsymbol{\Phi}_{1_0} = \begin{bmatrix} 62.696 & 25.499 \\ 25.499 & 21.687 \end{bmatrix},$$

$$\boldsymbol{\Phi}_{2_0} = \begin{bmatrix} 11154.919 & 7235.158 \\ 7235.158 & 11075.499 \end{bmatrix}.$$

The state responses of the NN and the released time intervals of SDDETM 1 and SDDETM 2 when $N_1 = N_2 \in \{0, 2, 4\}$ are depicted in Fig. 3. Total number of triggers released by SDDETM 1 and SDDETM 2 with different N_1 and N_2 values are presented in Table 2. The effectiveness of the designed DOFC in stabilizing the system can be obtained from the above results.

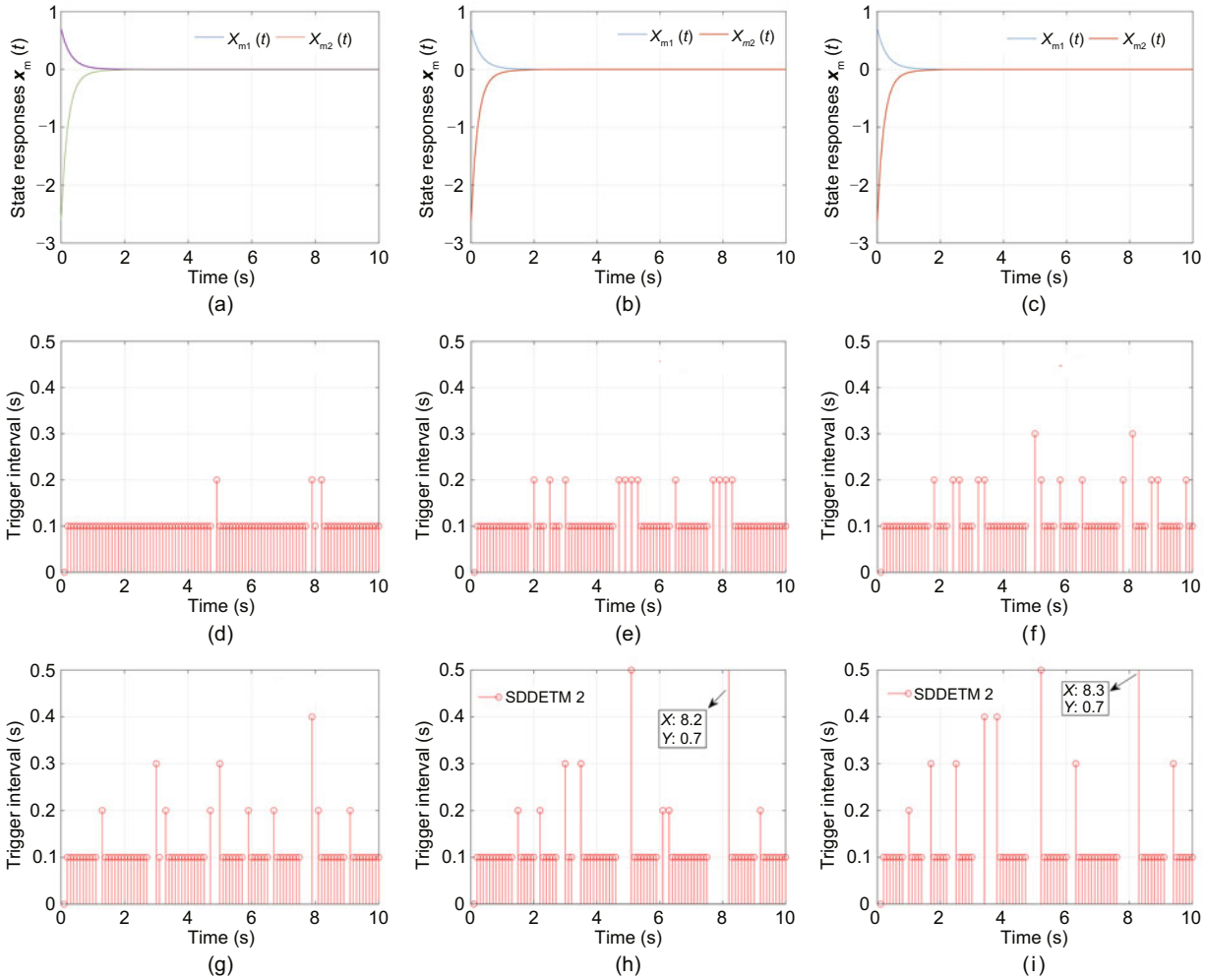

Fig. 3 The state trajectories and release time intervals of SDDETM 1 and SDDETM 2 in Case 2, for state trajectories with $N_1 = N_2 = 0$ (a), $N_1 = N_2 = 2$ (b), and $N_1 = N_2 = 4$ (c), for SDDETM 1 with $N_1 = N_2 = 0$ (d), $N_1 = N_2 = 2$ (e), $N_1 = N_2 = 4$ (f), and for SDDETM 2 with $N_1 = N_2 = 0$ (g), $N_1 = N_2 = 2$ (h), and $N_1 = N_2 = 4$ (i)

Table 2 Total triggers generated by SDDETM with different N_1 and N_2 values in Case 2

$N_1 = N_2$	N_{trigger}			ϵ_{1_i} $(i \in \mathcal{N}_{N_1})$	ϵ_{2_j} $(j \in \mathcal{N}_{N_2})$
	SDDETM 1	SDDETM 2	Total		
0 (Tan et al., 2020)	86	82	168	0.05	0.05
1	82	77	159	0.05, 0.15	0.05, 0.25
2	80	76	156	0.05, 0.15, 0.30	0.05, 0.25, 0.40
3	74	74	148	0.05, 0.15, 0.30, 0.30	0.05, 0.25, 0.40, 0.40
4	72	72	144	0.05, 0.15, 0.30, 0.30, 0.30	0.05, 0.25, 0.40, 0.40, 0.40
$N_1 = N_2$	N_{trigger}			ϵ_{1_i} $(i \in \mathcal{N}_{N_1})$	ϵ_{2_j} $(j \in \mathcal{N}_{N_2})$
	SDDETM 1	SDDETM 2	Total		
0 (Tan et al., 2020)	86	82	168	0.05	0.05
1	83	79	162	0.05, 0.10	0.05, 0.25
2	82	78	160	0.05, 0.10, 0.15	0.05, 0.25, 0.25
3	80	76	156	0.05, 0.10, 0.15, 0.20	0.05, 0.25, 0.25, 0.40
4	78	74	152	0.05, 0.10, 0.15, 0.20, 0.30	0.05, 0.25, 0.25, 0.40, 0.40

N_{trigger}: number of triggers

5 Conclusions

The objective of this paper is to design a DOFC and an SDDETM to ensure the synchronization of master and slave NNs under deception attacks. The proposed SDDETM offers significant advantages over traditional ETMs by reducing trigger frequency, avoiding Zeno behavior, and providing more efficient use of network resources. Through the application of the CCL algorithm, the concurrent design of the DOFC and SDDETM parameters is achieved, further enhancing the stability and performance of the system. The simulation results validate the effectiveness of the proposed SDDETM in achieving faster and more stable convergence compared to traditional ETMs.

Future research should consider the design under conditions where multi-packet transmission and disorder are common, as the current work assumes that packets are transmitted individually and orderly.

Contributors

Zhongjing YU and Duo ZHANG designed the research. Zhongjing YU processed the data. Zhongjing YU and Duo ZHANG drafted the paper. Shihan KONG, Deqiang OUYANG, and Hongfei LI helped organize the paper. Junzhi YU revised and finalized the paper.

Conflict of interest

All the authors declare that they have no conflict of interest.

Data availability

The data that support the findings of this study are available from the corresponding authors upon reasonable request.

References

Bao YG, Zhao D, Sun JY, et al., 2024. Resilient synchronization of neural networks under DoS attacks and communication delays via event-triggered impulsive control. *IEEE Trans Syst Man Cybern Syst*, 54(1):471-483. https://doi.org/10.1109/TSMC.2023.3312520

Boyd S, El Ghaoui L, Feron E, et al., 1994. Linear Matrix Inequalities in System and Control Theory. https://doi.org/10.1137/1.9781611970777

Chen J, Zhang XM, Park JH, et al., 2022. Improved stability criteria for delayed neural networks using a quadratic function negative-definiteness approach. *IEEE Trans Neur Netw Learn Syst*, 33(3):1348-1354. https://doi.org/10.1109/TNNLS.2020.3042307

Donkers MCF, Heemels WPMH, 2012. Output-based event-triggered control with guaranteed $\mathcal{L}_\infty$-gain and improved and decentralized event-triggering. *IEEE Trans Autom Contr*, 57(6):1362-1376. https://doi.org/10.1109/TAC.2011.2174696

El Ghaoui L, Oustry F, AitRami M, 1997. A cone complementarity linearization algorithm for static output-feedback and related problems. *IEEE Trans Autom Contr*, 42(8):1171-1176. https://doi.org/10.1109/9.618250

Guo G, Ding L, Han QL, 2014. A distributed event-triggered transmission strategy for sampled-data consensus of multi-agent systems. *Automatica*, 50(5):1489-1496. https://doi.org/10.1016/j.automatica.2014.03.017

Heemels WPMH, Donkers MCF, Teel AR, 2013. Periodic event-triggered control for linear systems. *IEEE Trans Autom Contr*, 58(4):847-861. https://doi.org/10.1109/TAC.2012.2220443

Kazemy A, Lam J, Zhang XM, 2022. Event-triggered output feedback synchronization of master–slave neural networks under deception attacks. *IEEE Trans Neur Netw Learn Syst*, 33(3):952-961. https://doi.org/10.1109/TNNLS.2020.3030638

Lei Y, Hua T, Wang YW, et al., 2024. Robust output regulation of singularly perturbed systems by event-triggered output feedback. *IEEE Trans Syst Man Cybern Syst*, 54(4):2104-2113. https://doi.org/10.1109/TSMC.2023.3334204

Liang D, Huang J, 2021. Robust output regulation of linear systems by event-triggered dynamic output feedback control. *IEEE Trans Autom Contr*, 66(5):2415-2422. https://doi.org/10.1109/TAC.2020.3010772

Liu JL, Wei LL, Xie XP, et al., 2018. Quantized stabilization for T–S fuzzy systems with hybrid-triggered mechanism and stochastic cyber-attacks. *IEEE Trans Fuzzy Syst*, 26(6):3820-3834. https://doi.org/10.1109/TFUZZ.2018.2849702

Liu JL, Yin TT, Xie XP, et al., 2019a. Event-triggered state estimation for T–S fuzzy neural networks with stochastic cyber-attacks. *Int J Fuzzy Syst*, 21(2):532-544. https://doi.org/10.1007/s40815-018-0590-4

Liu JL, Gu YY, Xie XP, et al., 2019b. Hybrid-driven-based H_∞ control for networked cascade control systems with actuator saturations and stochastic cyber attacks. *IEEE Trans Syst Man Cybern Syst*, 49(12):2452-2463. https://doi.org/10.1109/TSMC.2018.2875484

Liu YJ, Fang Z, Park JH, et al., 2023. Quantized event-triggered synchronization of discrete-time chaotic neural networks with stochastic deception attack. *IEEE Trans Syst Man Cybern Syst*, 53(7):4511-4521. https://doi.org/10.1109/TSMC.2023.3251355

Liu ZQ, Lou XY, Jia JJ, 2022. Event-triggered dynamic output-feedback control for a class of Lipschitz nonlinear systems. *Front Inform Technol Electron Eng*, 23(11):1684-1699. https://doi.org/10.1631/FITEE.2100552

Ma YJ, Wang Y, Li ZJ, et al., 2024. Event-triggered finite-time command-filtered tracking control for nonlinear time-delay cyber physical systems against cyber attacks. *Front Inform Technol Electron Eng*, 25(2):225-236. https://doi.org/10.1631/FITEE.2300613

Shen H, Liu YA, Wang J, et al., 2023. Sliding-mode control for IT2 fuzzy nonlinear singularly perturbed systems and its application to electric circuits: a dynamic event-triggered mechanism. *IEEE Trans Syst Man Cybern Syst*, 53(7):4077-4090. https://doi.org/10.1109/TSMC.2023.3240994

Song L, Nguang SK, Huang D, 2019. Hierarchical stability conditions for a class of generalized neural networks with multiple discrete and distributed delays. *IEEE Trans Neur Netw Learn Syst*, 30(2):636-642. https://doi.org/10.1109/tnnls.2018.2853658

Tan YS, Liu Y, Niu B, et al., 2020. Event-triggered synchronization control for T–S fuzzy neural networked systems with time delay. *J Franklin Inst*, 357(10):5934-5953. https://doi.org/10.1016/j.jfranklin.2020.03.024

Wang R, Li YH, Sun H, et al., 2021. Freshness constraints of an age of information based event-triggered Kalman consensus filter algorithm over a wireless sensor network. *Front Inform Technol Electron Eng*, 22(1):51-67. https://doi.org/10.1631/FITEE.2000206

Wen GH, Chen MZQ, Yu XH, 2016. Event-triggered master–slave synchronization with sampled-data communication. *IEEE Trans Circ Syst II Expr Briefs*, 63(3):304-308. https://doi.org/10.1109/TCSII.2015.2482158

Wen GH, Wan Y, Cao JD, et al., 2018. Master–slave synchronization of heterogeneous systems under scheduling communication. *IEEE Trans Syst Man Cybern Syst*, 48(3):473-484. https://doi.org/10.1109/TSMC.2016.2599012

Yan S, Shen MQ, Nguang SK, et al., 2019. A distributed delay method for event-triggered control of T–S fuzzy networked systems with transmission delay. *IEEE Trans Fuzzy Syst*, 27(10):1963-1973. https://doi.org/10.1109/TFUZZ.2019.2893179

Yue D, Tian EG, Han QL, 2013. A delay system method for designing event-triggered controllers of networked control systems. *IEEE Trans Autom Contr*, 58(2):475-481. https://doi.org/10.1109/TAC.2012.2206694

Zadeh LA, 1968. Fuzzy algorithms. *Inform Contr*, 12(2):94-102. https://doi.org/10.1016/S0019-9958(68)90211-8

Zhang D, Ouyang D, Shu L, et al., 2023. Sum-based event-triggered dynamic output feedback control for synchronization of fuzzy neural networks with deception attacks. *Neur Comput Appl*, 35(14):10221-10237. https://doi.org/10.1007/s00521-023-08231-7

Zhang LR, Nguang SK, Ouyang DQ, et al., 2020. Synchronization of delayed neural networks via integral-based event-triggered scheme. *IEEE Trans Neur Netw Learn Syst*, 31(12):5092-5102. https://doi.org/10.1109/TNNLS.2019.2963146

Zhang LR, Nguang SK, Yan S, 2021. Event-triggered H_∞ control for networked control systems under denial-of-service attacks. *Trans Inst Meas Contr*, 43(5):1077-1087. https://doi.org/10.1177/0142331220966417

Zhang XM, Han QL, 2014. Event-triggered dynamic output feedback control for networked control systems. *IET Contr Theory Appl*, 8(4):226-234. https://doi.org/10.1049/iet-cta.2013.0253

Zhang XM, Han QL, Wang J, 2018. Admissible delay upper bounds for global asymptotic stability of neural networks with time-varying delays. *IEEE Trans Neur Netw Learn Syst*, 29(11):5319-5329. https://doi.org/10.1109/TNNLS.2018.2797279